Diffusion and Kinetics

Lecture: Crystal Interfaces and Microstructure

Nikolai V. Priezjev

Crystal Interfaces and Microstructure

► Interfacial Free Energy

► Solid-Vapor Interfaces

► Boundaries in Single-Phase Solids

     (1) Low- & High-Angle Boundaries (2) Special Boundaries (3) Kinetics
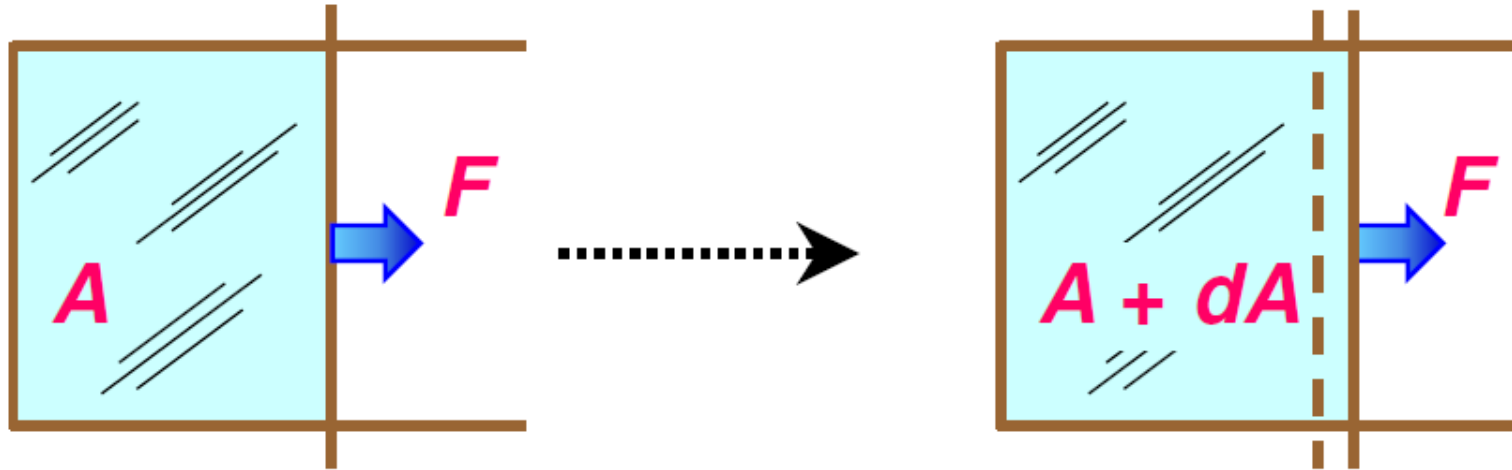
► Interphase Interfaces in Solids

► Interface Migration

Reading: Chapter 3 of Porter, Easterling, Sherif

Basic Interface Types

❑ **Free Surfaces** (solid / vapour interface)

❑ **Grain Boundaries** (α / α interface)

❑ **Interphase Interfaces** (α / β interface)

❑ **Metallographic Surfaces**

3.1 Interfacial Free Energy

liquid film

$$G = G_0 + A \gamma \qquad \gamma: \text{free energy per unit area}$$

$$dG = \gamma dA + A d\gamma = F dA \qquad (\text{word done by } F)$$

$$\text{if } \gamma = \text{const.}, \quad F = \gamma \quad (\text{surf. tension} = \text{surf. energy})$$
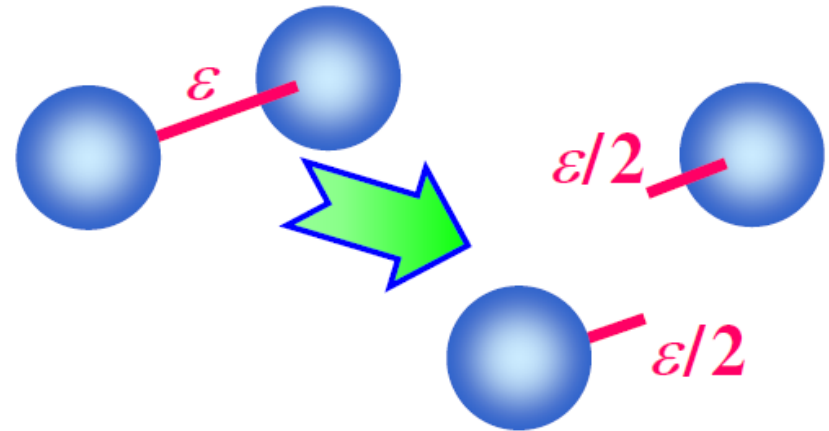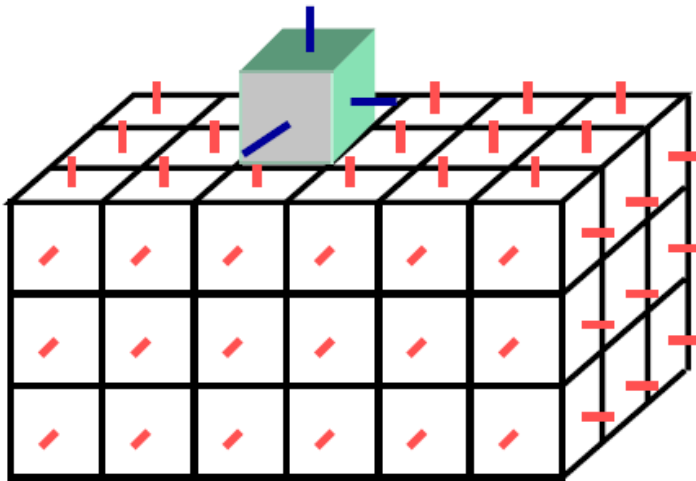
dimension: Jm^{-2}

Force per unit length!

3.2 Solid - Vapor Interfaces

what does the surface energy originate from?

—— **broken bonds**

$$L_s = Z N_a \varepsilon / 2$$
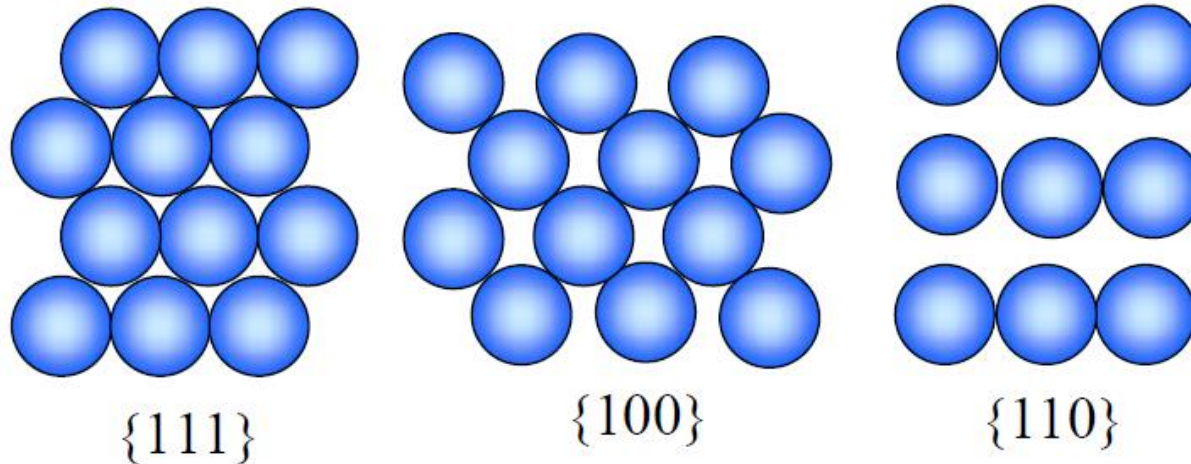
L_s : sublimation heat

Z : number of nearest neighbors

N_a : Avogadro's number

$$= 6.022 \times 10^{23} \text{ mol}^{-1}$$

3.2 Solid - Vapor Interfaces

directional dependence of the surface energy in crystals: the number of broken bonds in an fcc crystal increases from {111} to {100} to {110} faces and, in general, H_s can be expected to be higher for high {hkl} index of the crystal face.

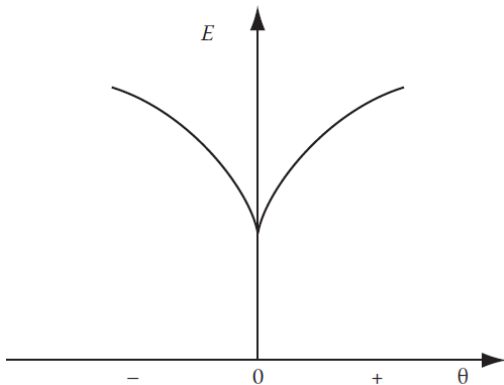{111}   {100}   {110}

High-indexed surface

higher or irrational $\{hkl\}$ index ?

stepped layers of close-packed planes

unit length

$1/a$

$(\sin|\theta|)/a$ broken bonds

θ

$\rightarrow a \leftarrow$
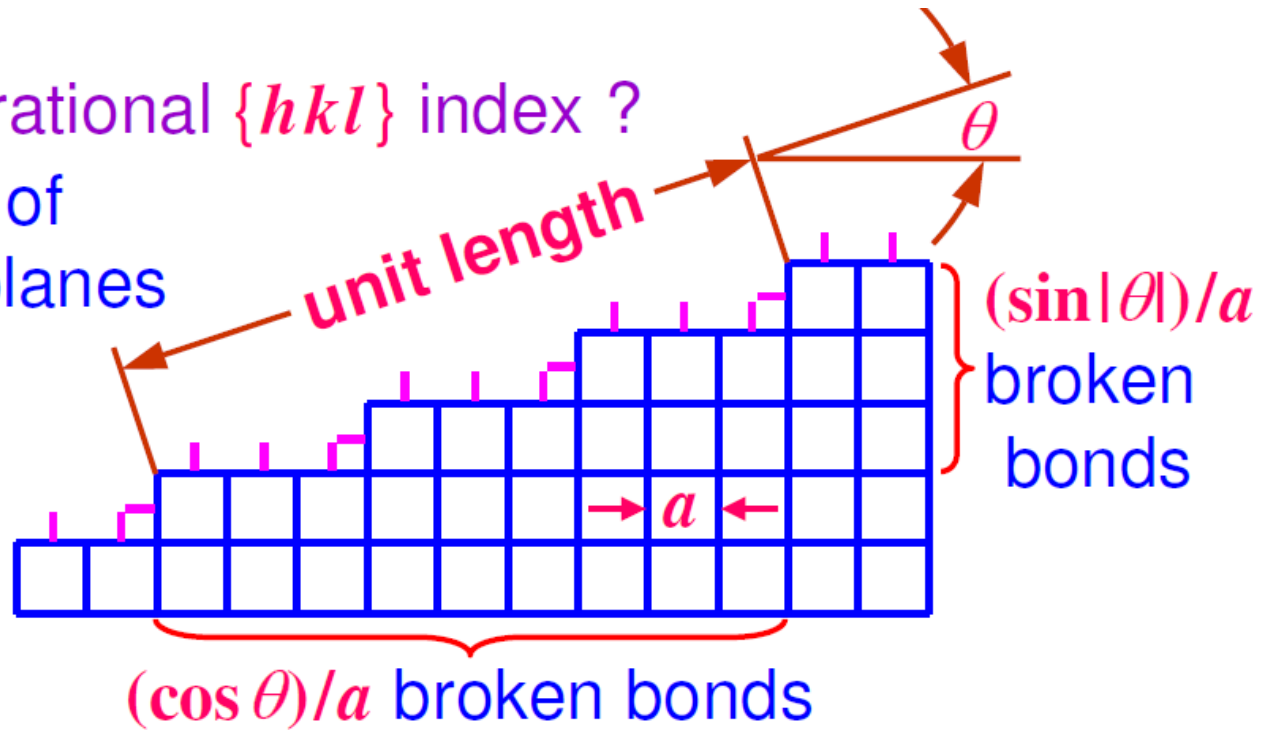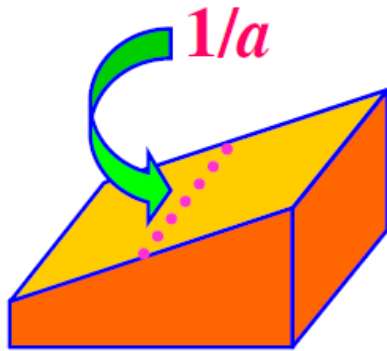
$(\cos\theta)/a$ broken bonds

broken bonds per unit surface with a crystal plane at an angle θ to the close-packed plane:

$$(\cos\theta + \sin|\theta|)/a^2$$

$$E_{sv} = (\cos\theta + \sin|\theta|)\cdot\varepsilon/2a^2$$

Variation of surface energy as a function of ➜

High-indexed surface: γ - plot

A Wulff plane

(001)

γ plot

surface in real space
normal to *OA*

A

B

$\gamma_{(001)}$

γ_A

(111)   (b)

γ-plot of a section in
3D orientation space

C

$\gamma_{(111)}$

(110)

0

Equilibrium
shape

(a)

Figure 3.5

(a) A possible $(\bar{1}10)$ section through the γ-plot of an fcc crystal. The length OA represents the free energy of a surface plane whose normal lies in the direction OA. Thus OB = $\gamma_{(001)}$, OC = $\gamma_{(111)}$ etc. Wulff planes are those such as that which lies normal to the vector OA. In this case the Wulff planes at the cusps (B, C, etc.) give the inner envelope of all Wulff planes and thus the equilibrium shape, (b) The equilibrium shape in three dimensions showing {100} (square faces) and {111} (hexagonal faces).
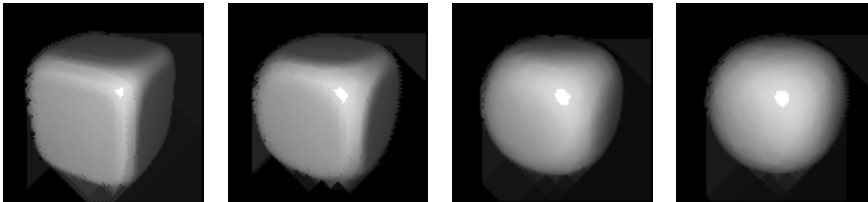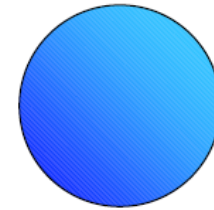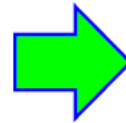
Equilibrium Crystal Surfaces
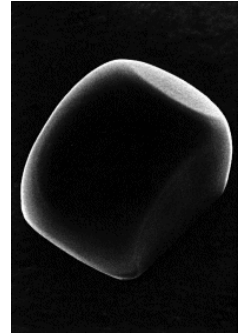
Surface Equilibrium of a Isolated Particle

a) **surfaces with lower energies**
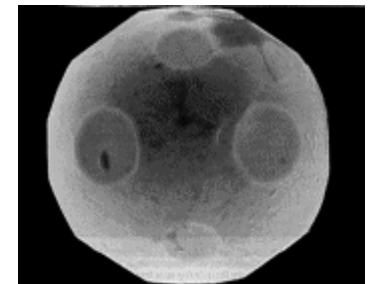specially oriented surfaces
(close-packed orientations)
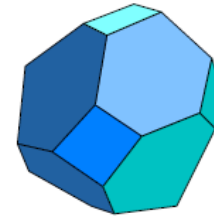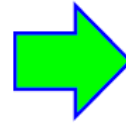
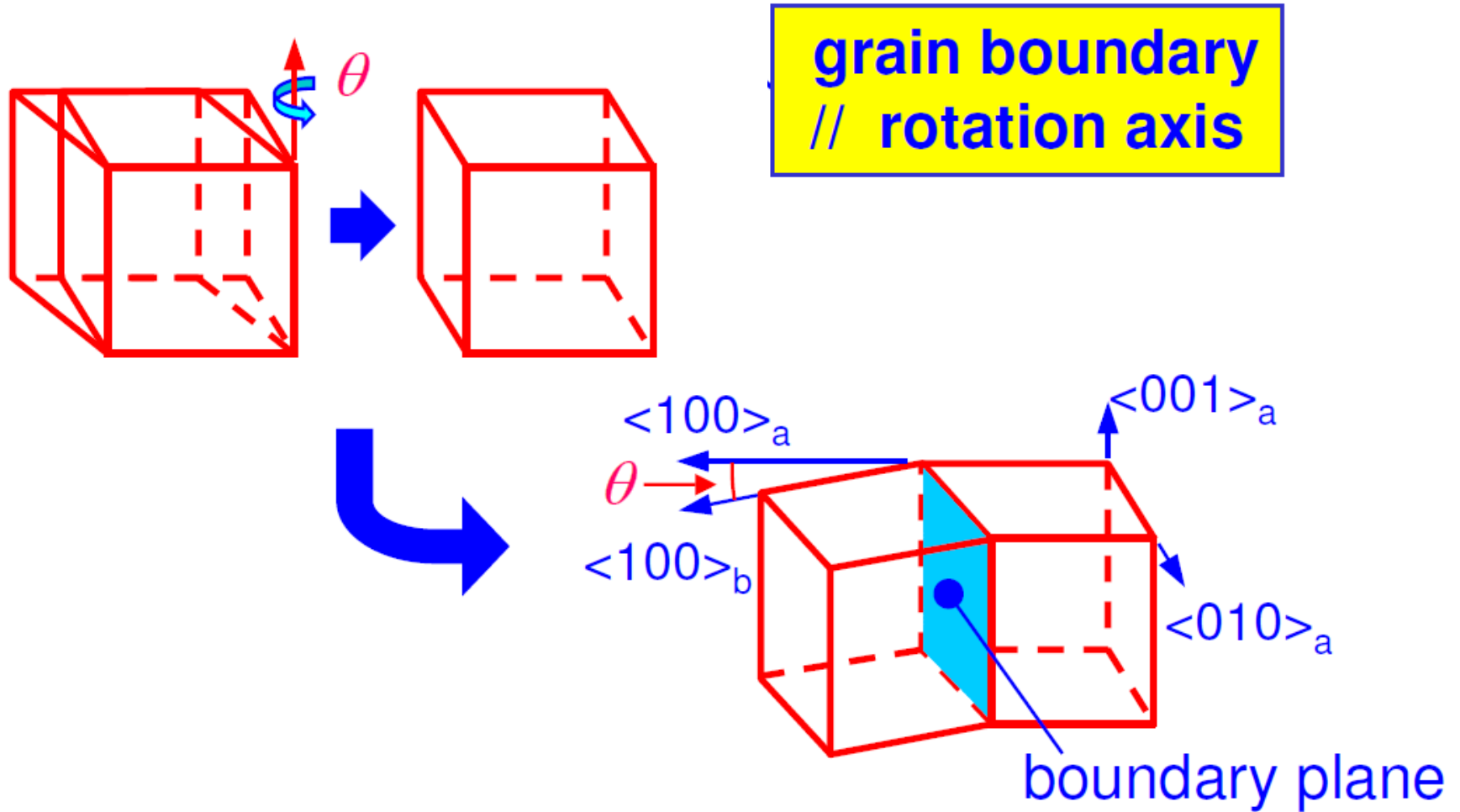**b)** **reduction of the total surface**
tending to a sphere

A salt crystal (NaCl), at 710 C. The six faces along the crystal lattice directions are flat

A gold crystal at about 1000 C

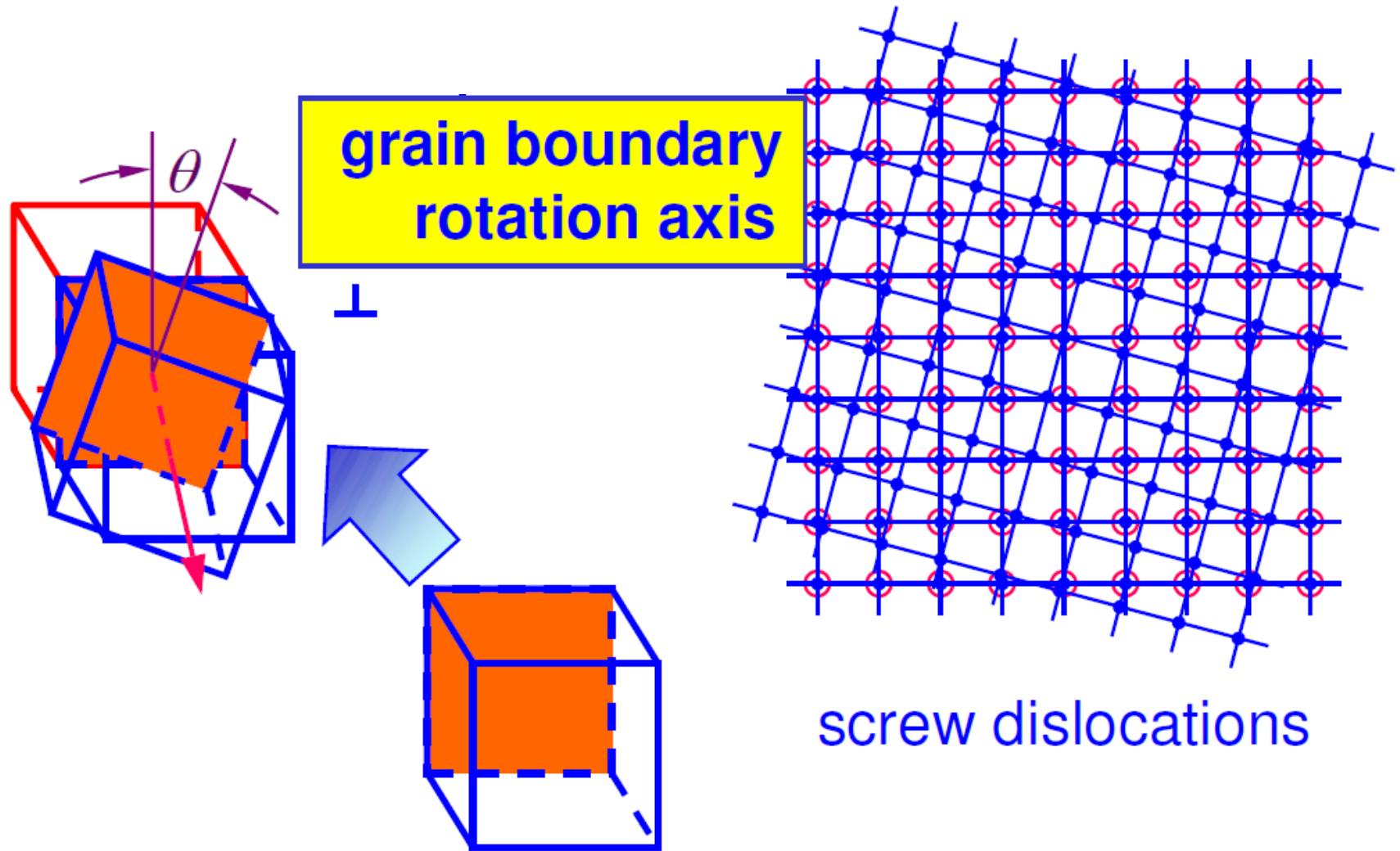Heating up to the roughening transition.

3.3 Boundaries in Single-Phase Solids: Tilt boundaries

grain boundary
// rotation axis

$<100>_a$

θ

$<100>_b$

$<001>_a$

$<010>_a$

boundary plane

3.3 Low-angle tilt boundaries

Top view:

$$D = \frac{b}{\tan \theta} \approx \frac{b}{\theta}$$
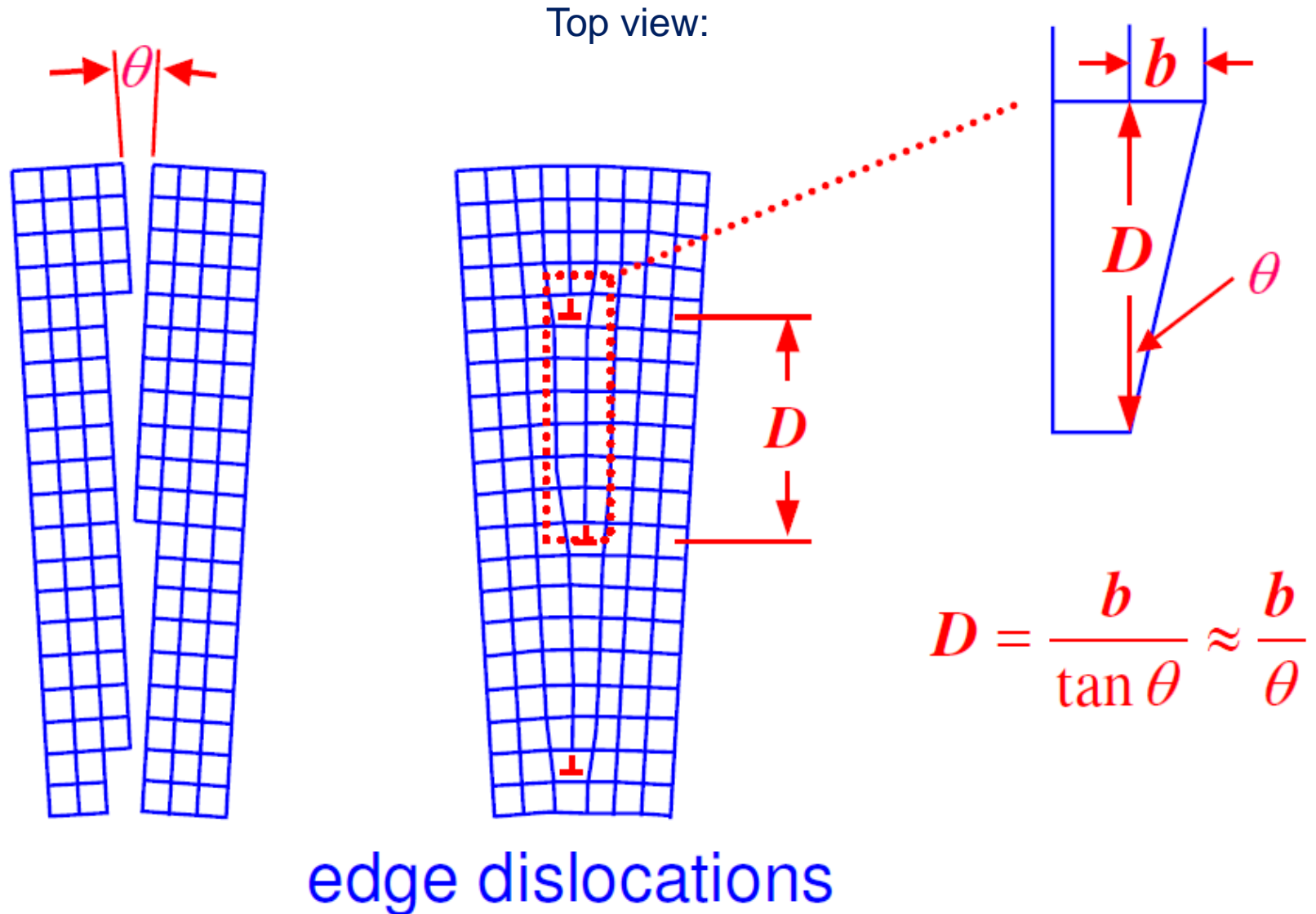
edge dislocations

3.3 Boundaries in Single-Phase Solids: Twist boundaries

θ

grain boundary
rotation axis
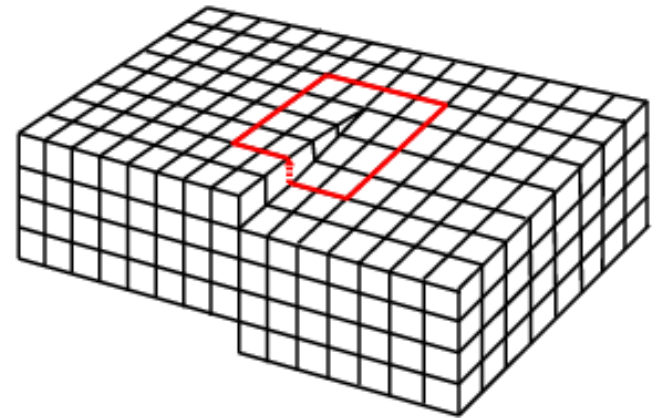
$\perp$

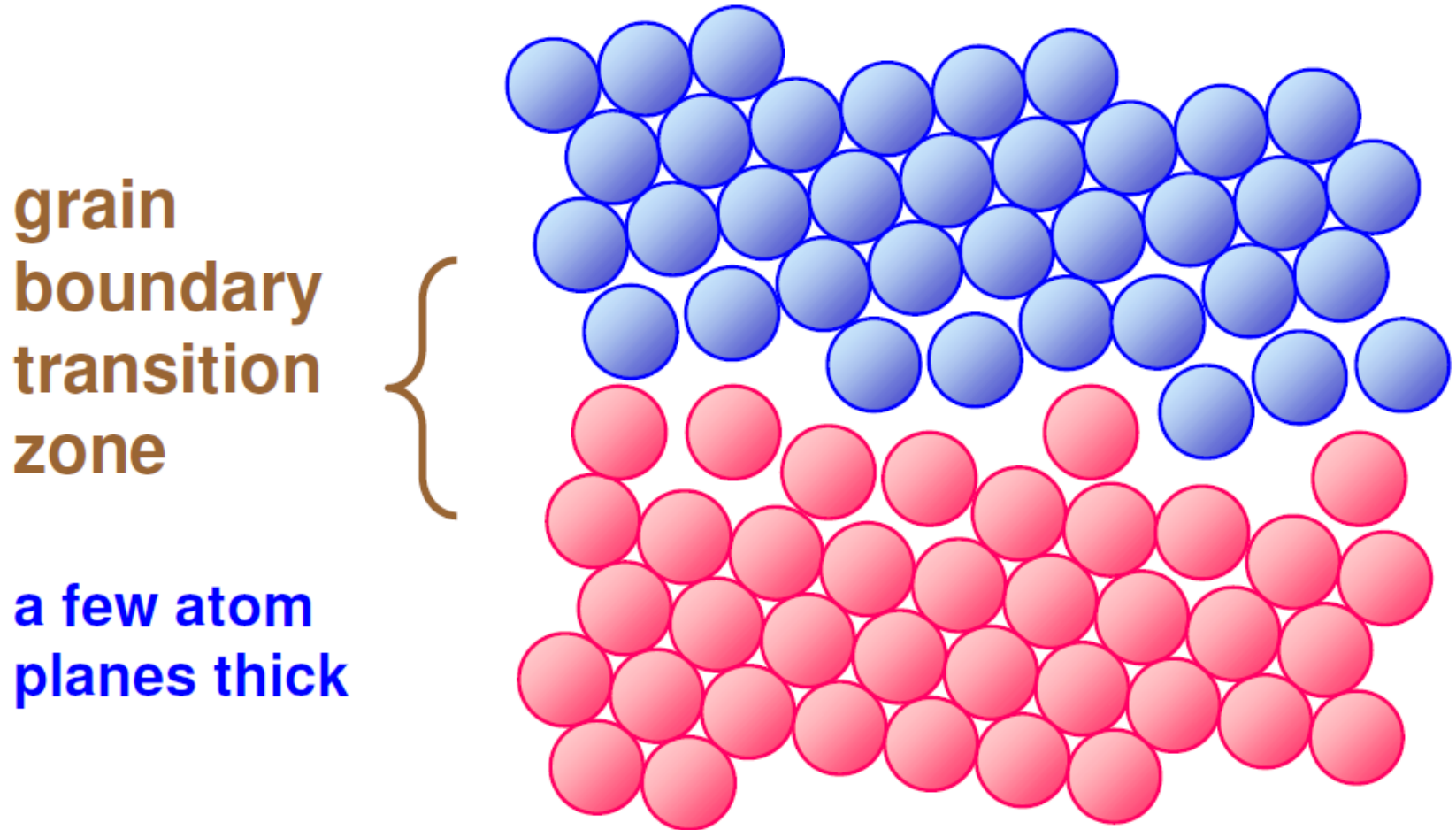screw dislocations

3.3 Low-Angle Twist boundaries
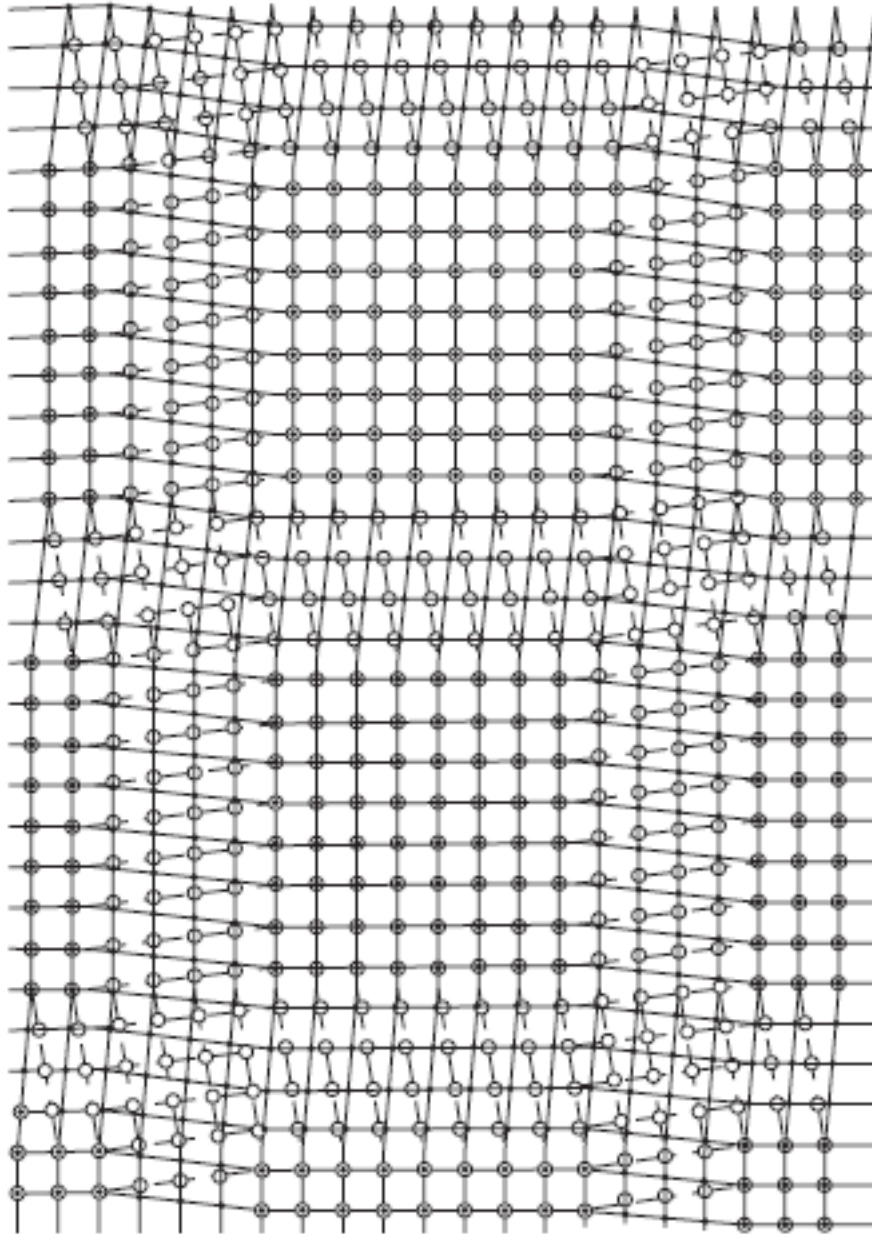
low-angle twist boundary:
○ atoms in crystal below
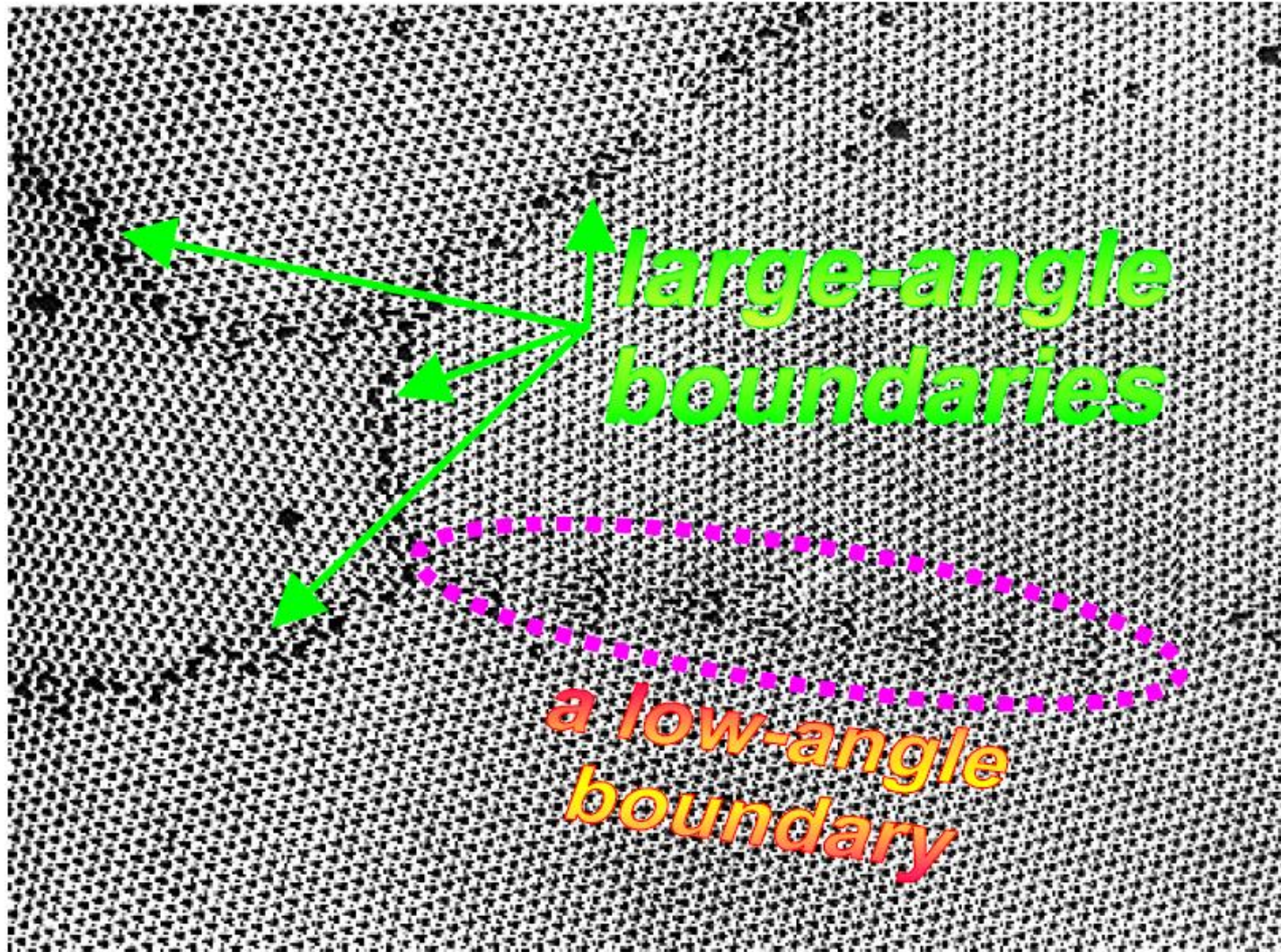boundary,   • atoms in
crystal above boundary.

Screw dislocation

Large-angle grain boundaries

grain
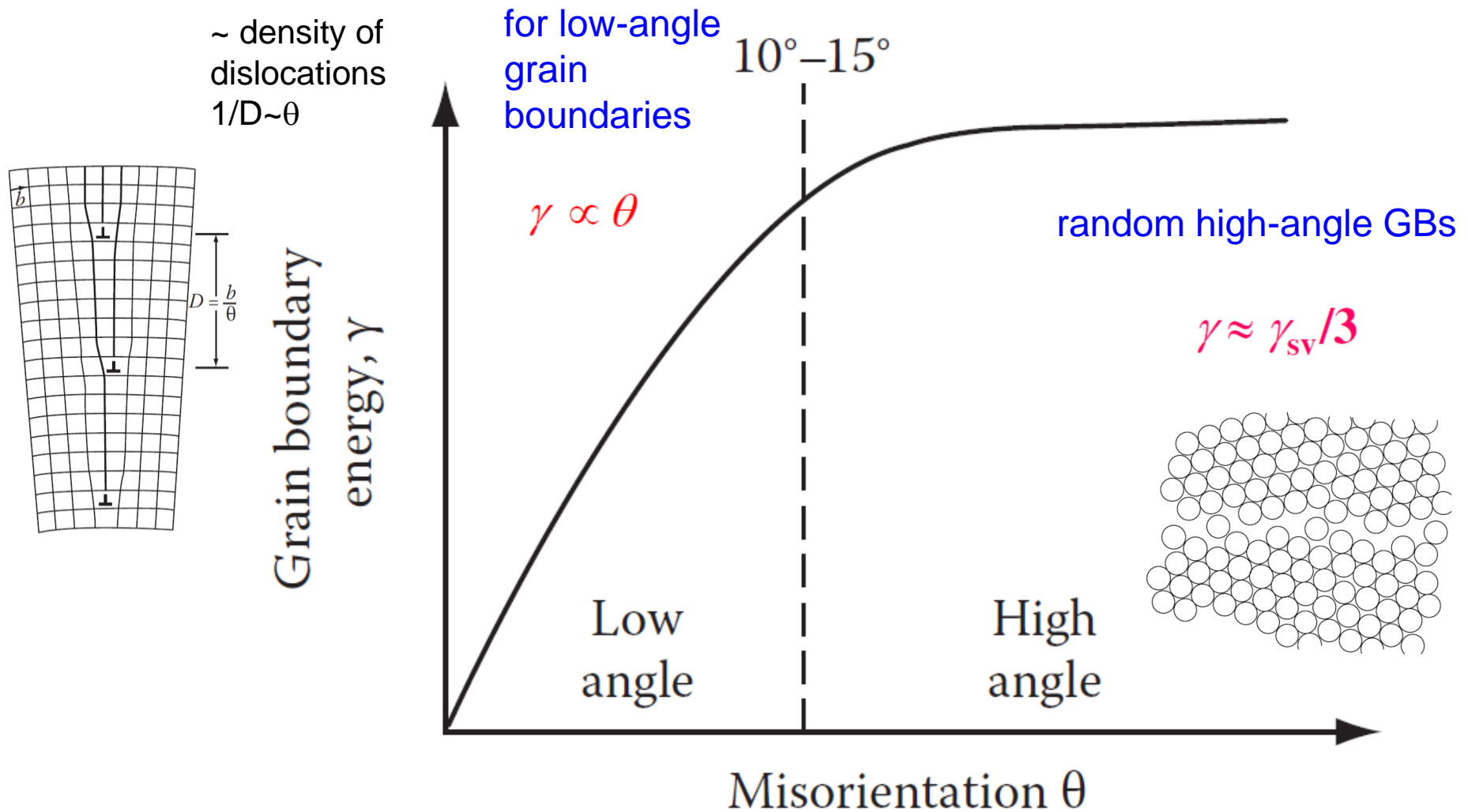boundary
transition
zone

a few atom
planes thick

Disordered grain boundary structure (schematic).

# Large- & low-angle boundaries

Rafts of soap bubbles showing several grains of varying misorientation. Note that the boundary with the smallest misorientation is made up of a row of dislocations, whereas the high-angle boundaries have a disordered structure in which individual dislocations cannot be identified.

# 3.3 Misorientation and boundary energy

~ density of
dislocations
$1/D \sim \theta$

for low-angle grain boundaries

$10° – 15°$

$\gamma \propto \theta$

random high-angle GBs

$\gamma \approx \gamma_{sv}/3$

Grain boundary energy, γ

$D = \frac{b}{\theta}$

b

Low angle

High angle

Misorientation θ

Variation of grain boundary energy with misorientation (schematic).

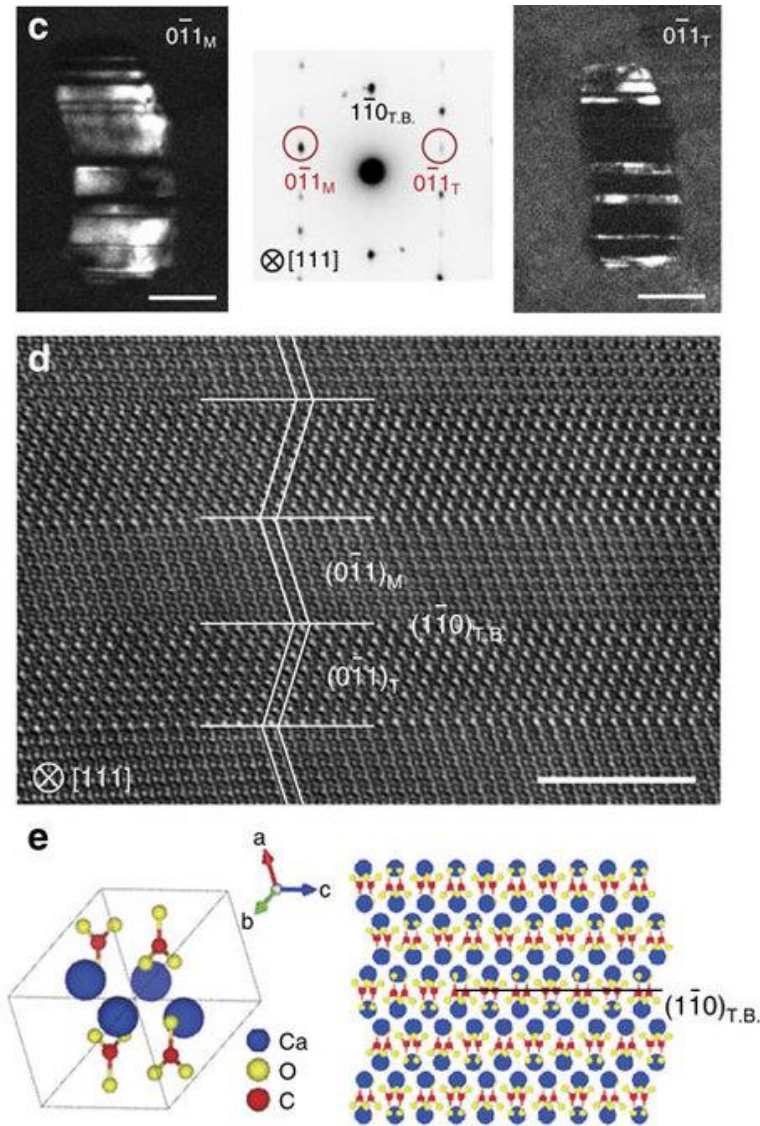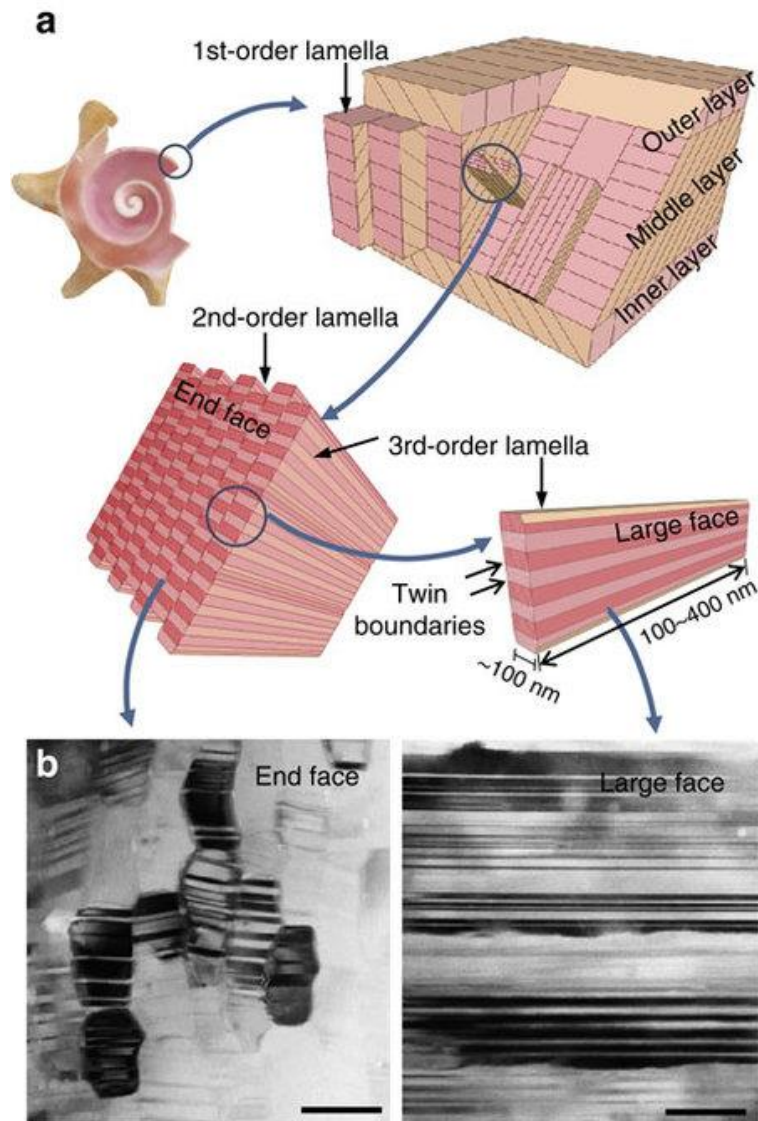# 3.3.2 Special Large-Angle Twin boundaries

a coherent twin boundary

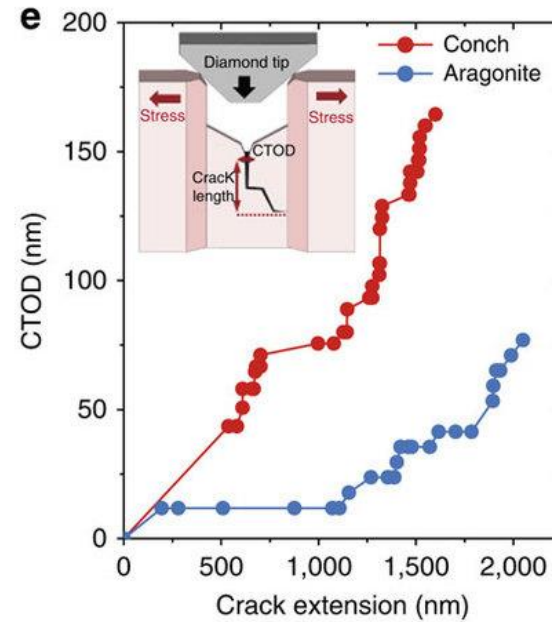an incoherent twin boundary
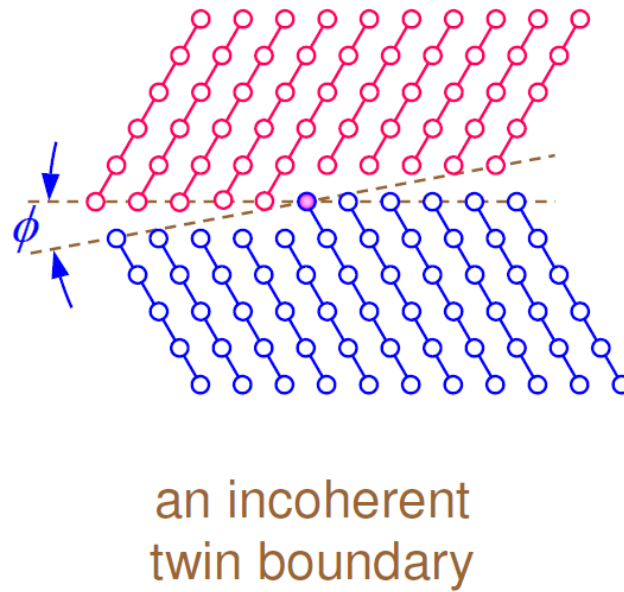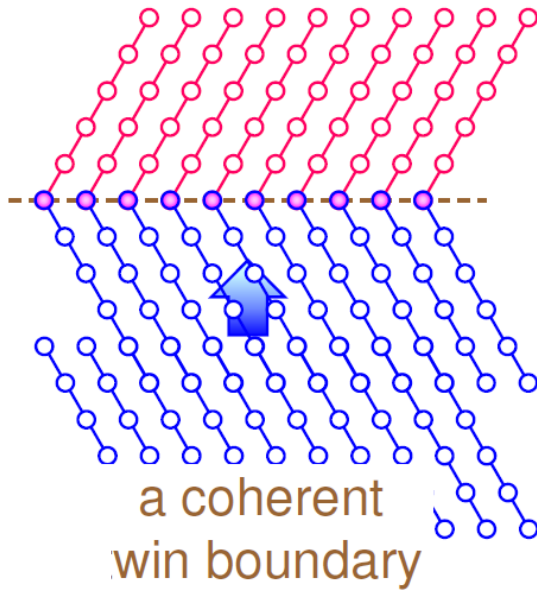
Twinned pyrite crystal group

Mirror symmetric structures
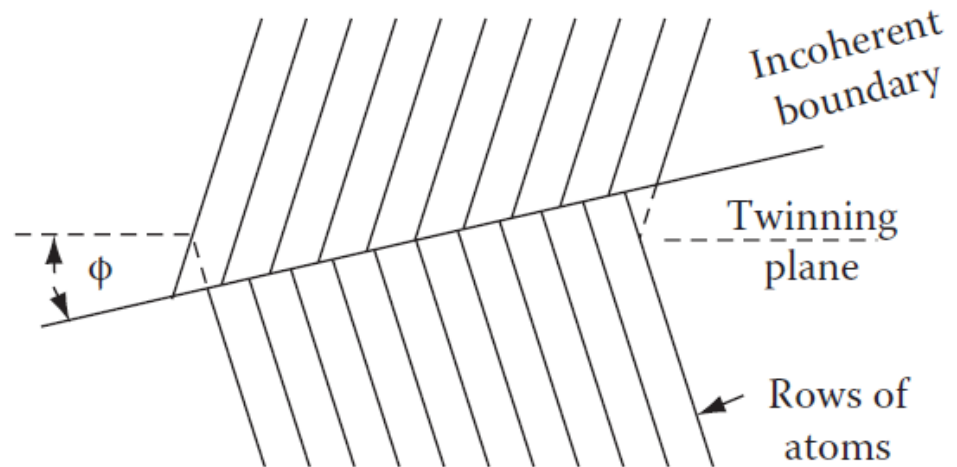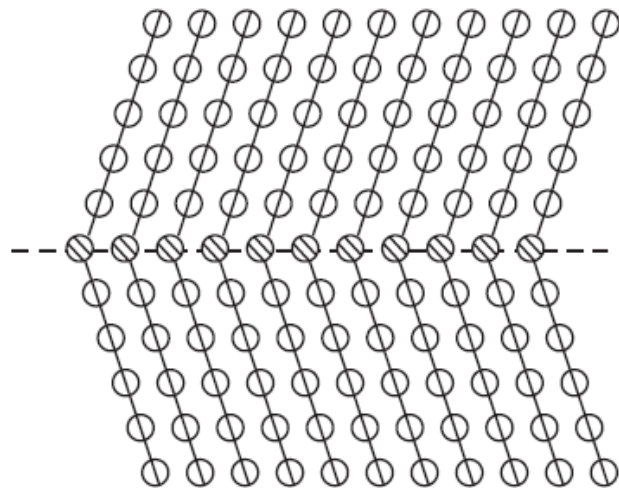
(a)

(b)

Incoherent boundary

Twinning plane

Rows of atoms

ϕ

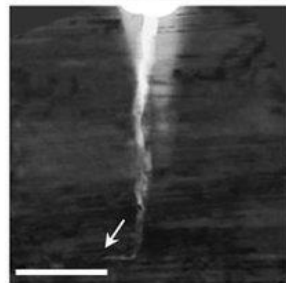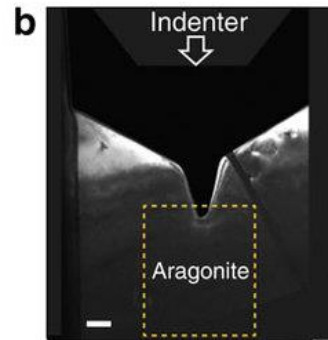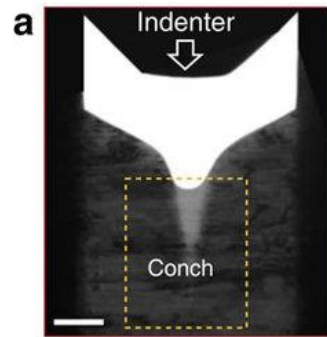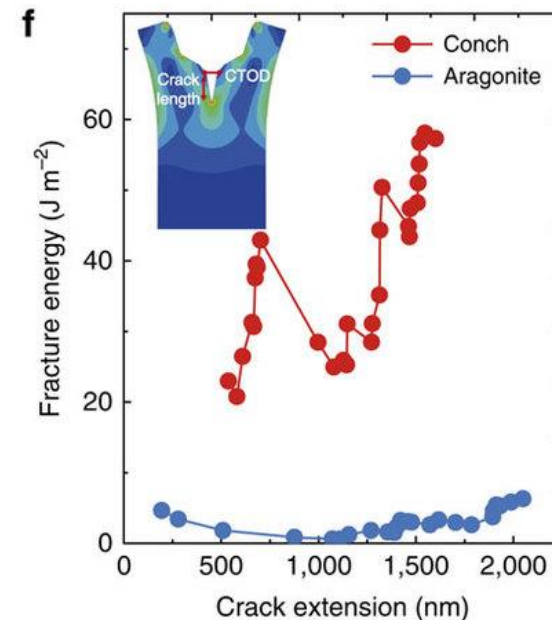# Nanotwin-governed toughening mechanism in hierarchically structured biological materials. Shin et al. Nature 2016

Nanotwin-governed toughening mechanism in hierarchically structured biological materials. Shin et al. Nature 2016

transmission electron microscope (TEM) images

aragonite single crystal: $CaCO_3$
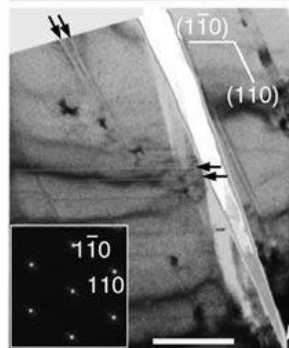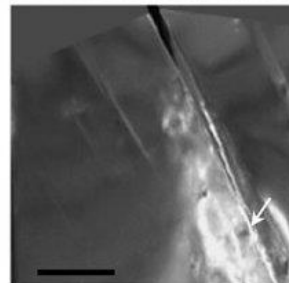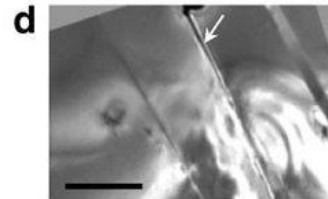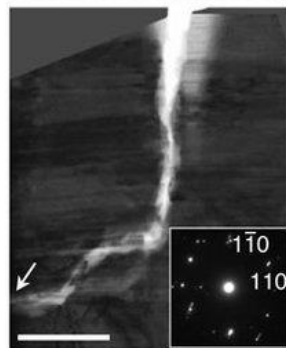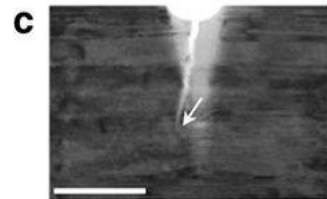
crack tip opening displacement (CTOD)

3.3.2 Special Large-Angle Twin boundaries

(a)

(b)

(c)

Incoherent twin

Coherent twin

Incoherent boundary

Twinning plane

Rows of atoms
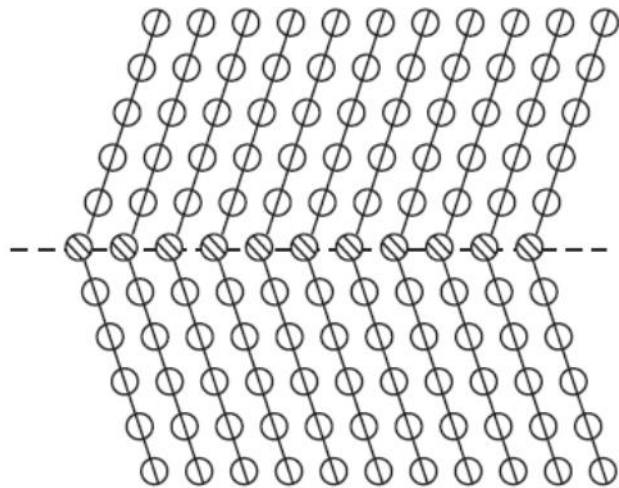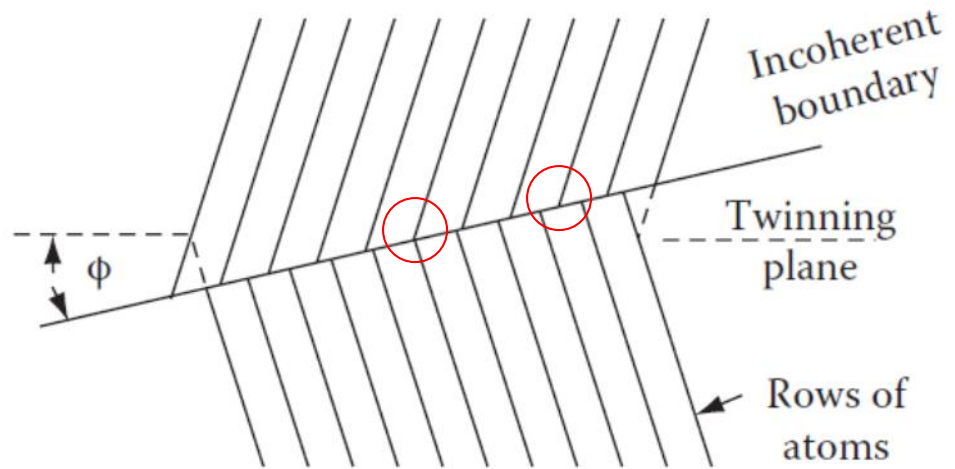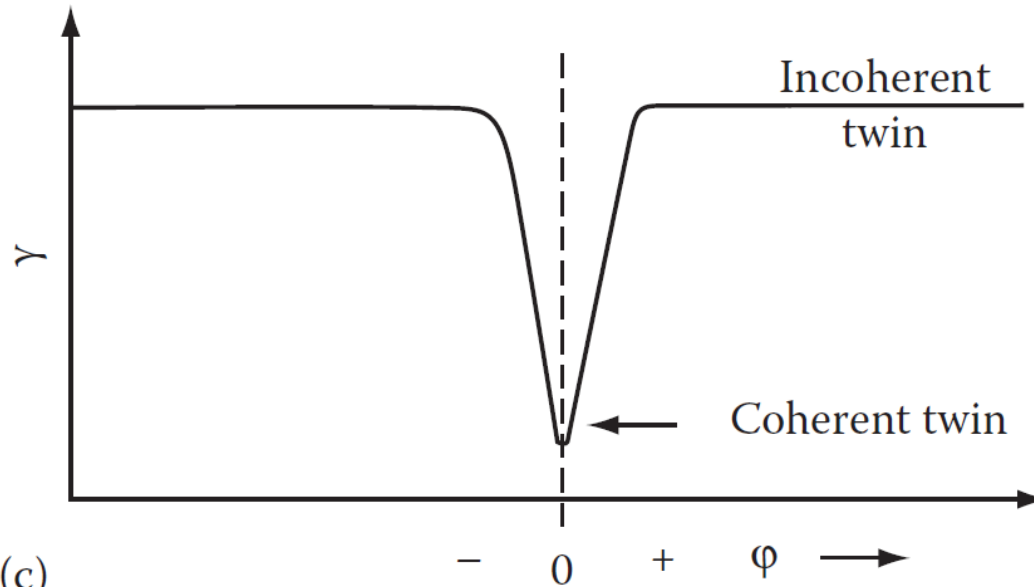
(a) A coherent twin boundary, (b) An incoherent twin boundary, (c) Twin-boundary energy as a function of the grain boundary orientation.

Mirror symmetric structures

3.3.2 Special Large-Angle Twin boundaries
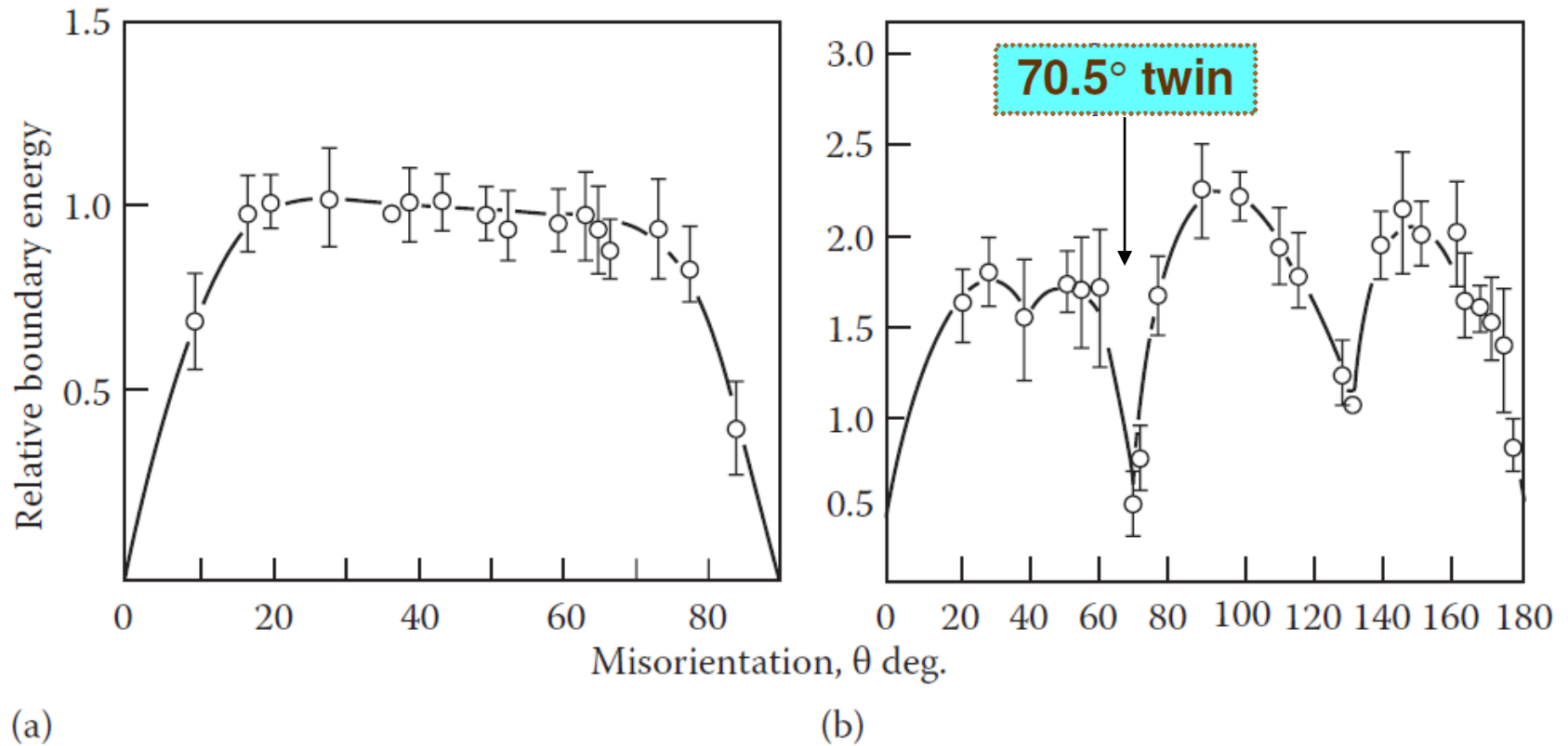
Measured grain boundary energies for symmetric tilt boundaries in Al FCC (a) when the rotation axis is parallel to ⟨100⟩, (b) when the rotation axis is parallel to ⟨110⟩.

Face Centered Cubic (FCC). Examples: Cu, Ag, Au, Ni, Pd, Pt, Al
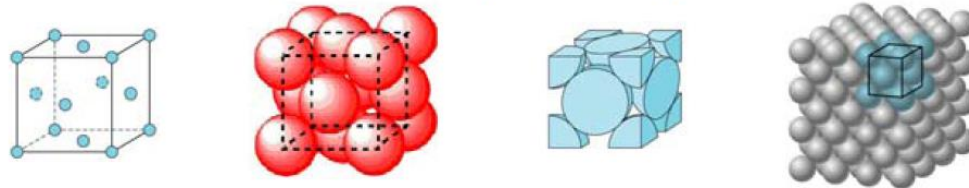
3.3.3 Equilibrium in Polycrystalline Materials
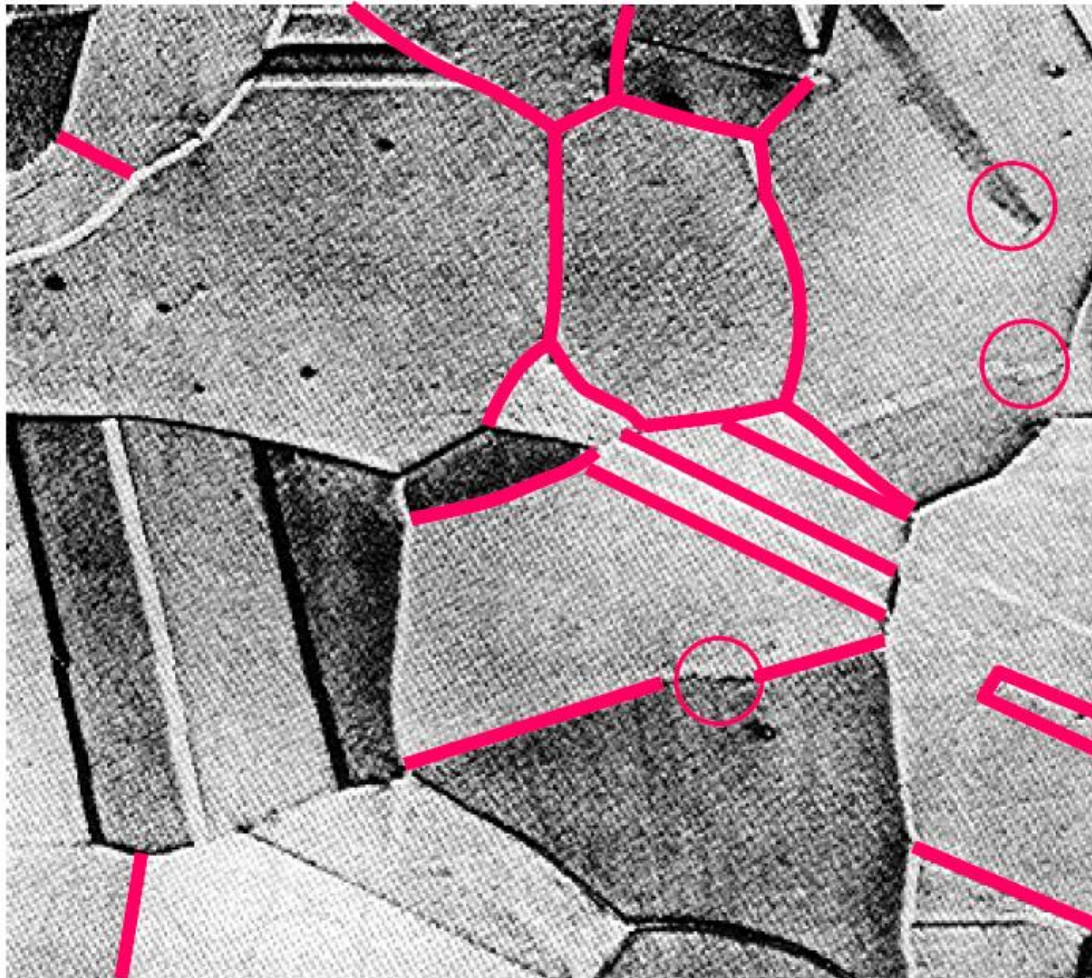
large-angle

low-angle

coherent twin

incoherent twin

Microstructure of an annealed crystal of austenitic stainless steel (fcc)

3.3.3 Grains and grain boundaries

Grains

—— 3D, but we see only sections

2 grains ➡ a grain boundary
a **line** in the section

3 grains ➡ a grain edge
a **triple-point** in the section

4 grains ➡ a grain corner
invisible in the section
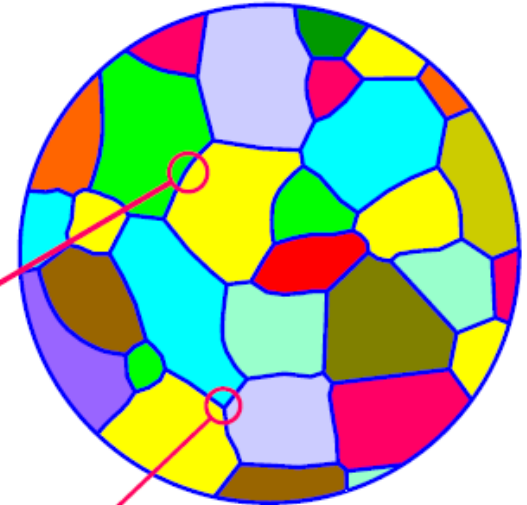
3.3.3 Grains and grain boundaries

why grain boundaries exist ?

GBs : high-energy regions in the structure, increase G relative to a single crystal

GBs : adjust themselves ➡ *metastable equilibrium*

important

- a GB could not stop in a grain
- GBs are generally mobile
- local equilibrium holds in GBs

3.3.3 Grains and grain boundaries
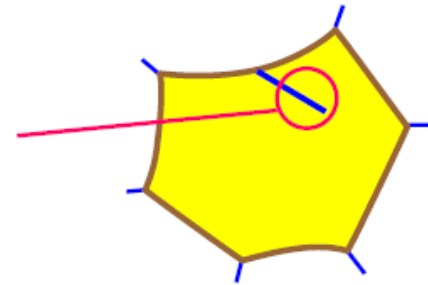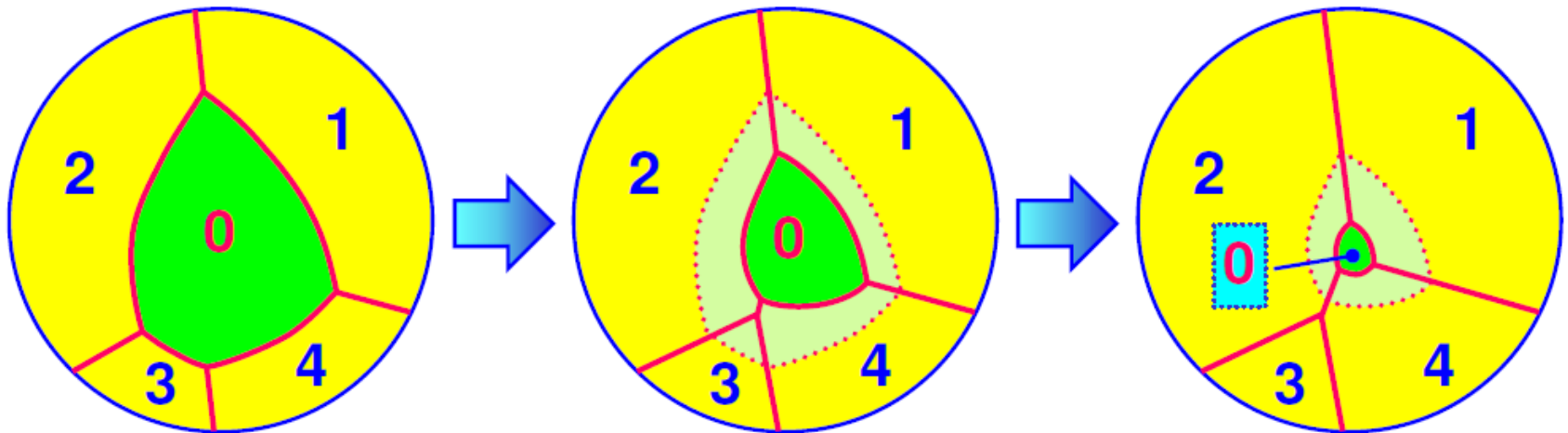
how could a boundary disappear ?

GBs : boundaries between different orientated grains could disappear only by the gradual migration

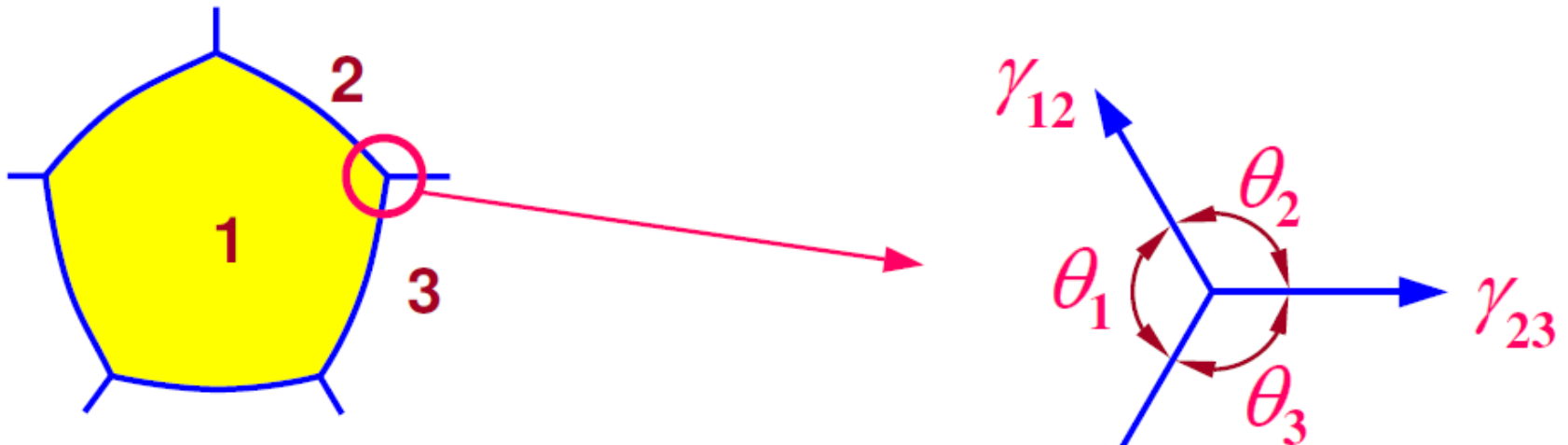- GBs' migration is coordinated with the triple points
- GBs' number remains constant if no grain disappear
- 3 GBs disappear when a grain disappear

Boundary Energy

➡ the equilibrium of GBs at triple points

γ : boundary energy, $\mathbf{J/m^2}$ (energy)
boundary tension, $\mathbf{N/m}$ (force)

$$\frac{\gamma_{23}}{\sin\theta_1} = \frac{\gamma_{31}}{\sin\theta_2} = \frac{\gamma_{12}}{\sin\theta_3}$$

3.3.3 Grains and grain boundaries: Curvature
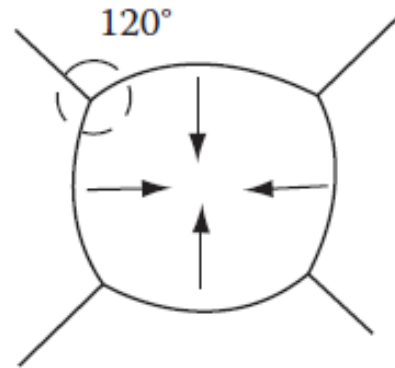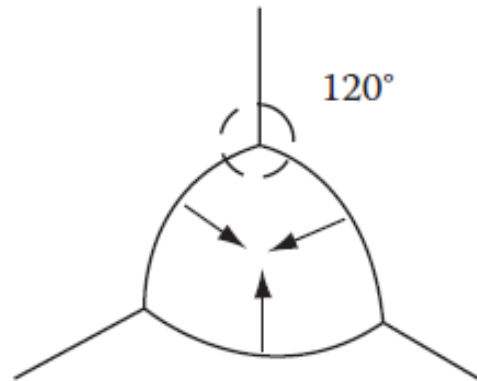
γ = const
θ = 120
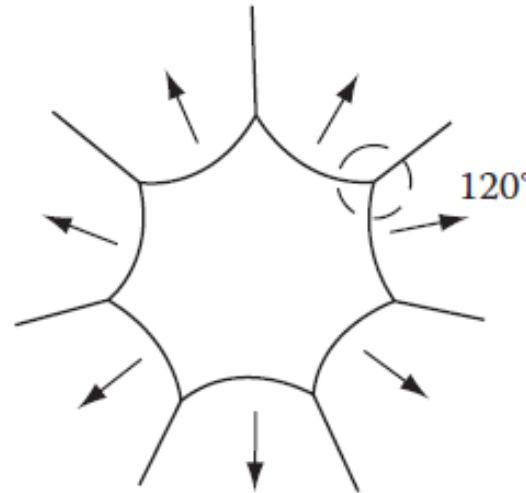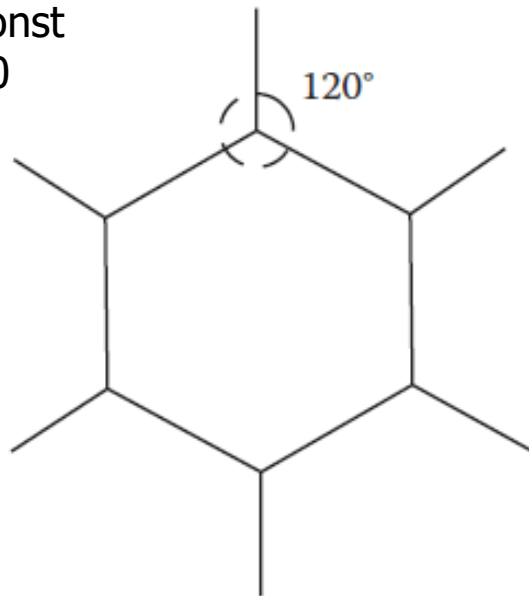
$$\Delta P = \frac{4\gamma}{R}$$

Two-dimensional grain boundary configurations. The arrows indicate the directions boundaries will migrate during grain growth. Grain coarsening.

3.3.3 Grains and grain boundaries: Curvature
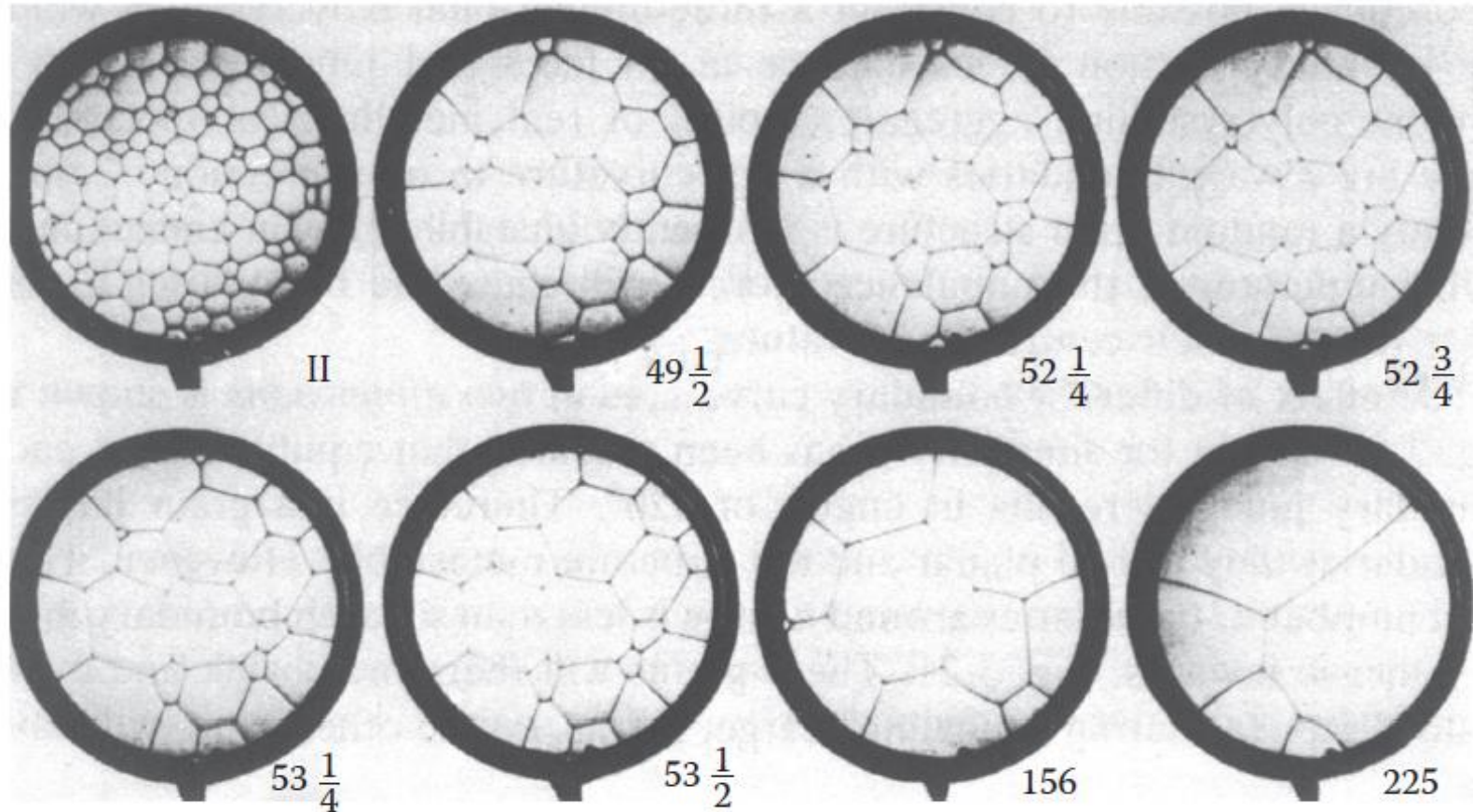
Two-dimensional cells of a soap solution illustrating the process of grain growth. Air molecules in smaller cells diffuse through film into the larger cells. Numbers are time in minutes.

3.3.3 Grains and grain boundaries: Topology

one cycle

✓ one grain vanished
✓ three boundaries disappeared
✓ the "5-7 pair" moves one step
✓ the average number of sides per grain keep constant ($n = 6$ for 2D systems)

3.3.4 Thermally Activated Migration of GB

Boundary motion

Grain 1   **Grain 2**

(a)   ⟵ δ ⟶
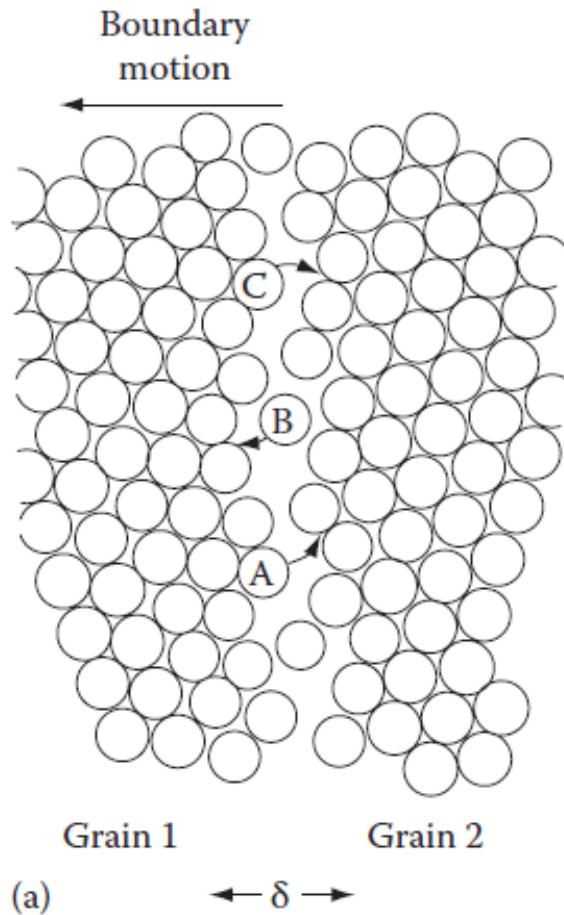
The atomic mechanism of boundary migration. The boundary migrates to the left if the jump rate from grain 1 → 2 is greater than 2 → 1. Note that the free volume within the boundary has been exaggerated for clarity.
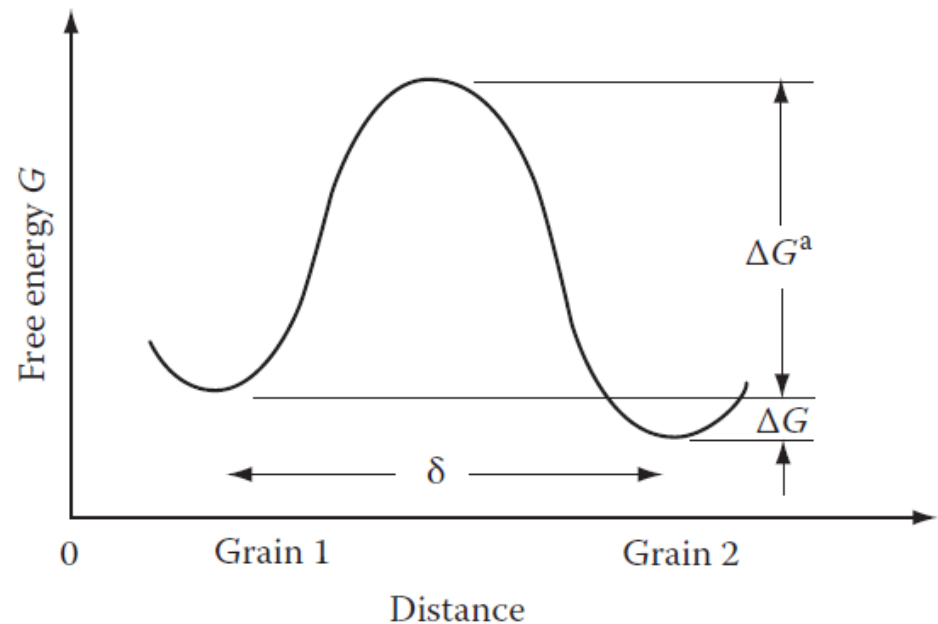
The free energy of an atom during the process of jumping from one grain to the other.

$$\Delta G_\gamma = \frac{2\gamma V_m}{r}$$

Gibbs-Thomson effect

$$v = M \cdot \Delta G_\gamma / V_m$$

3.3.5 Kinetics of Grain Growth

- **driving force of boundary migration**

  Laplace' Equation: $P = \gamma\left(\dfrac{1}{\rho_1} + \dfrac{1}{\rho_2}\right)$
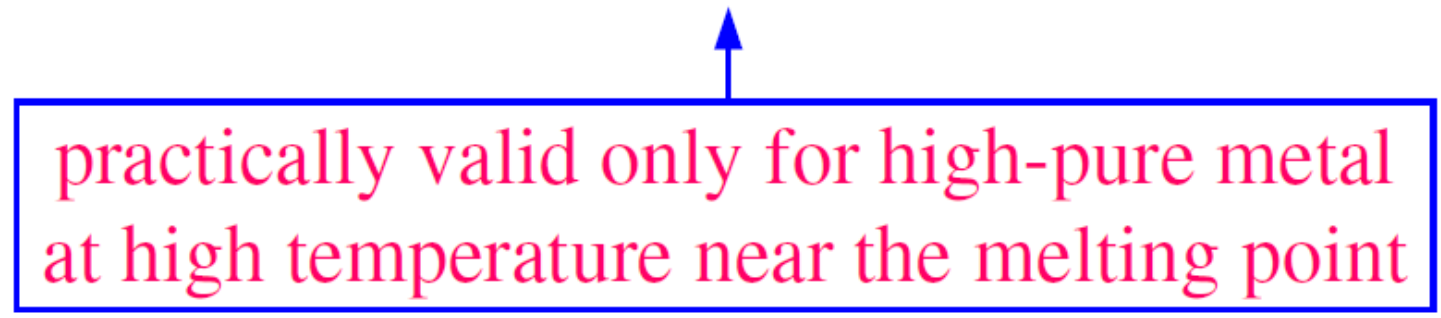
  boundary mobility

- **boundary migration rate**

  linear hypothesis: $v = mP$

  practically valid only for high-pure metal at high temperature near the melting point

3.3.5 Kinetics of Grain Growth

- grain growth rate ~ boundary migration rate

- boundary energy and mobility : constants

- boundary curvatures ~ grain sizes

$$\frac{d\overline{D}}{dt} \propto \overline{v} \propto \overline{mP} \propto m\gamma \cdot \overline{\left(\frac{1}{\rho_1} + \frac{1}{\rho_2}\right)} \propto 2m\gamma / \overline{D}$$

$$\frac{d\overline{D}}{dt} = \frac{2\alpha m\gamma}{\overline{D}} \implies \overline{D}^2 = \overline{D}_0^2 + 4\alpha m\gamma \cdot t$$

$$\implies \overline{D} = kt^{\eta}$$
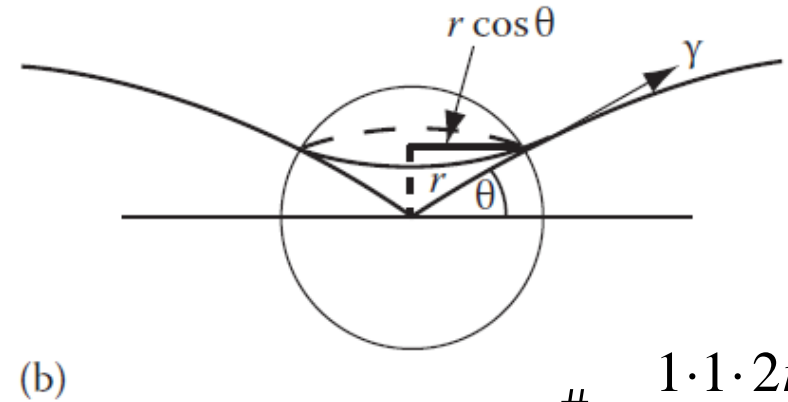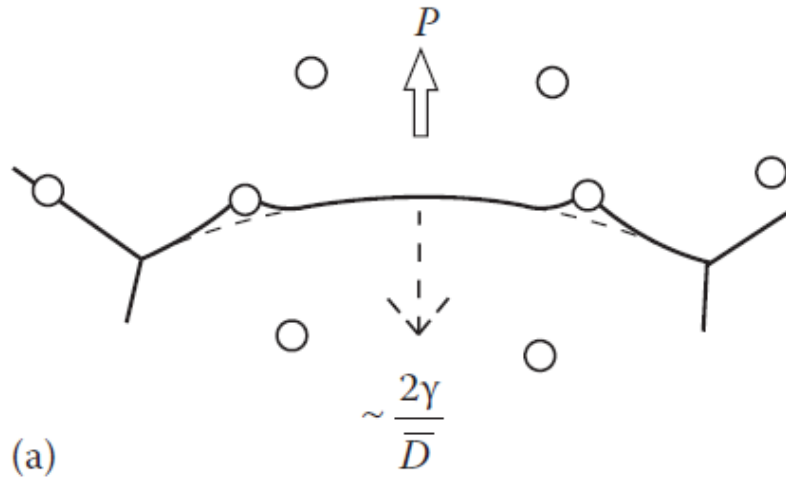
η: kinetic exponent

3.3.5 Kinetics of Grain Growth

Pure Me, high T
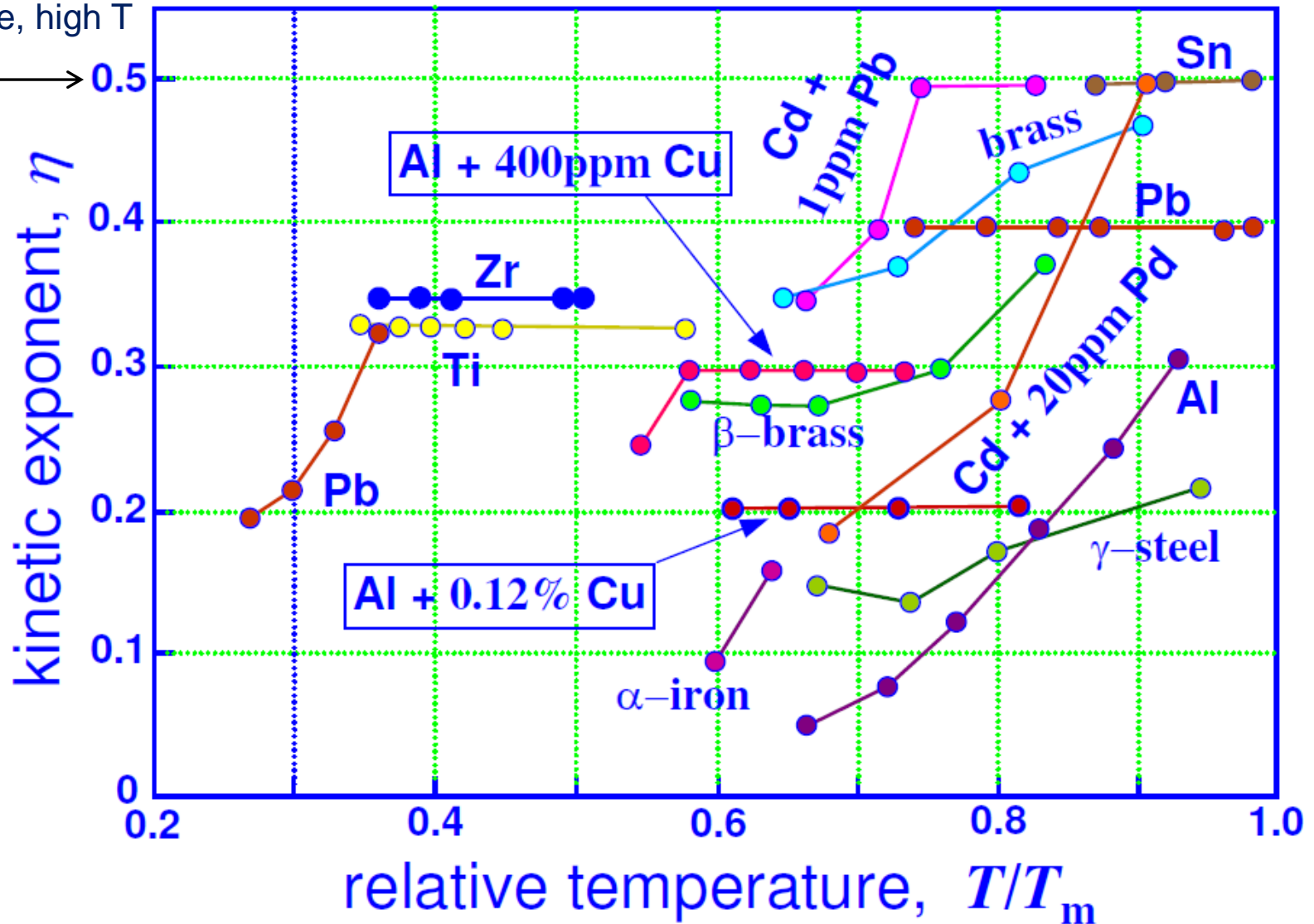
3.3.5 Kinetics of Grain Growth (in the presence of a second phase)

The effect of spherical particles on grain boundary migration

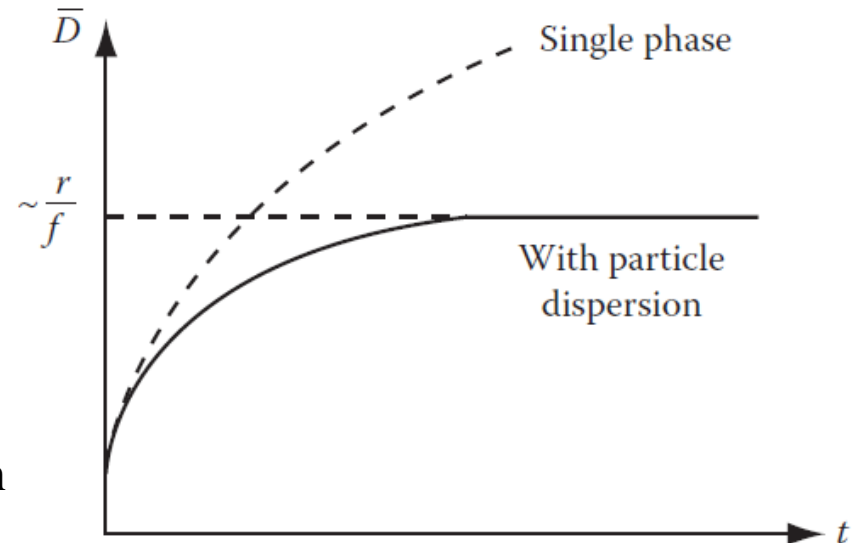$$\# = \frac{1 \cdot 1 \cdot 2r}{4/3 \cdot \pi r^3} f$$

Force from particle:

$$(2\pi r \cos\theta \, \gamma)\sin\theta = \pi r \gamma \quad (\theta = 45°)$$

$$P = \frac{3f}{2\pi r^2} \cdot \pi r \gamma = \frac{3f\gamma}{2r} \approx \frac{2\gamma}{\overline{D}}$$

$$\overline{D}_{max} = \frac{4r}{3f} \qquad f = \text{volume fraction of particles}$$

Effect of second-phase particles on grain growth

3.4 Interphase Interfaces in Solids

$$\gamma(\text{coherent}) = \gamma_{ch}$$

(a)

(b) A-B bonds
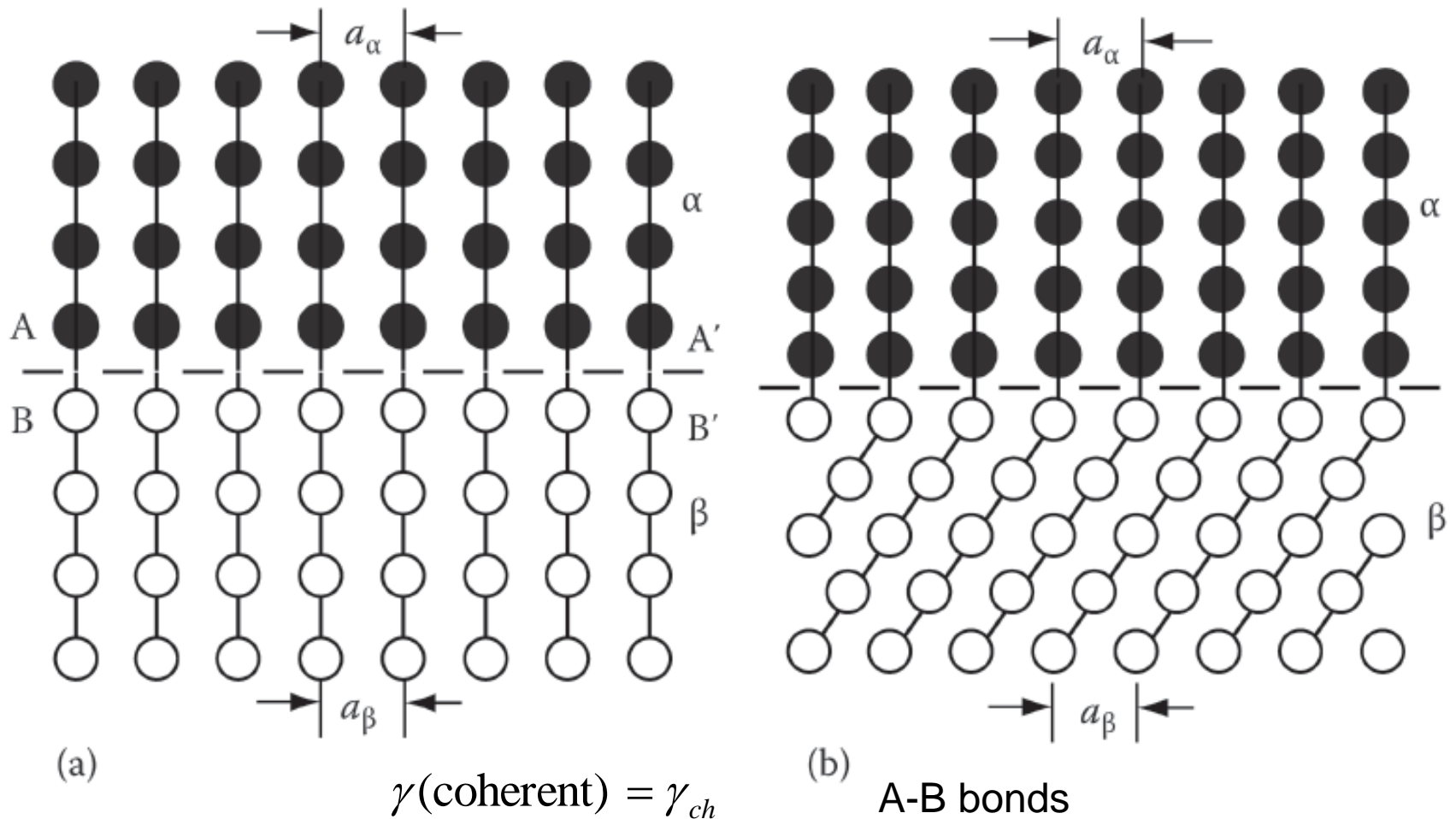
Strain-free <u>coherent interfaces</u>. (a) Each crystal has a different chemical composition but the same crystal structure. (b) The two phases have different lattices. Interfacial plane has the same atomic configuration in both phases, e.g., (111) fcc & (0001) hcp.

3.4 Interphase Interfaces in Solids
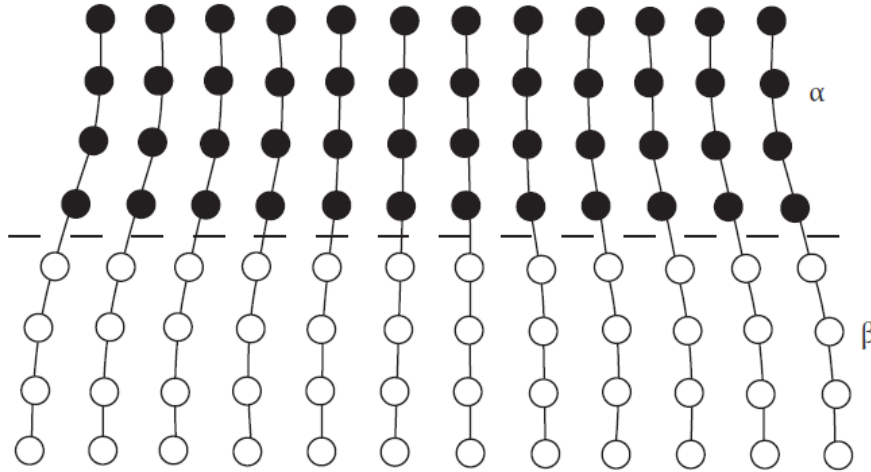
A <u>coherent interface</u> with slight mismatch leads to <u>coherency strains</u> (or lattice distortions) in the adjoining lattices.
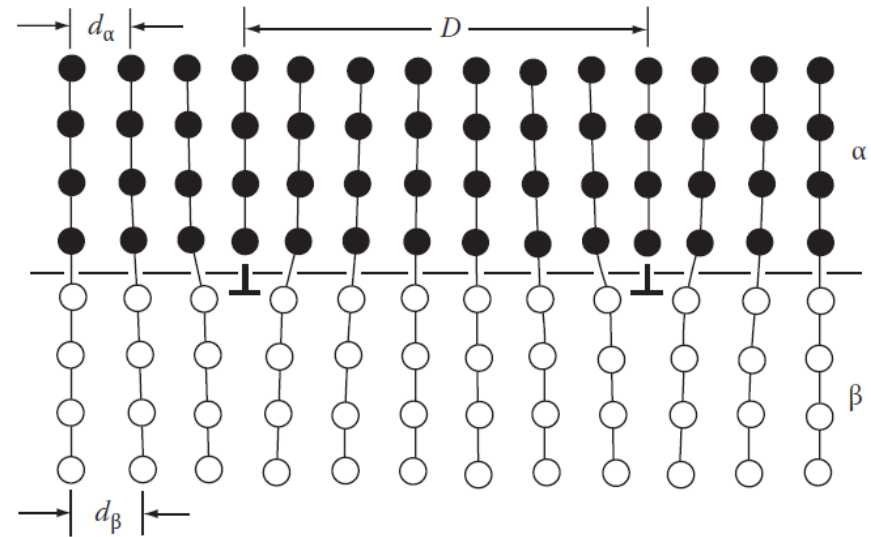
$$\gamma(\text{semicoherent}) = \gamma_{ch} + \gamma_{st}$$
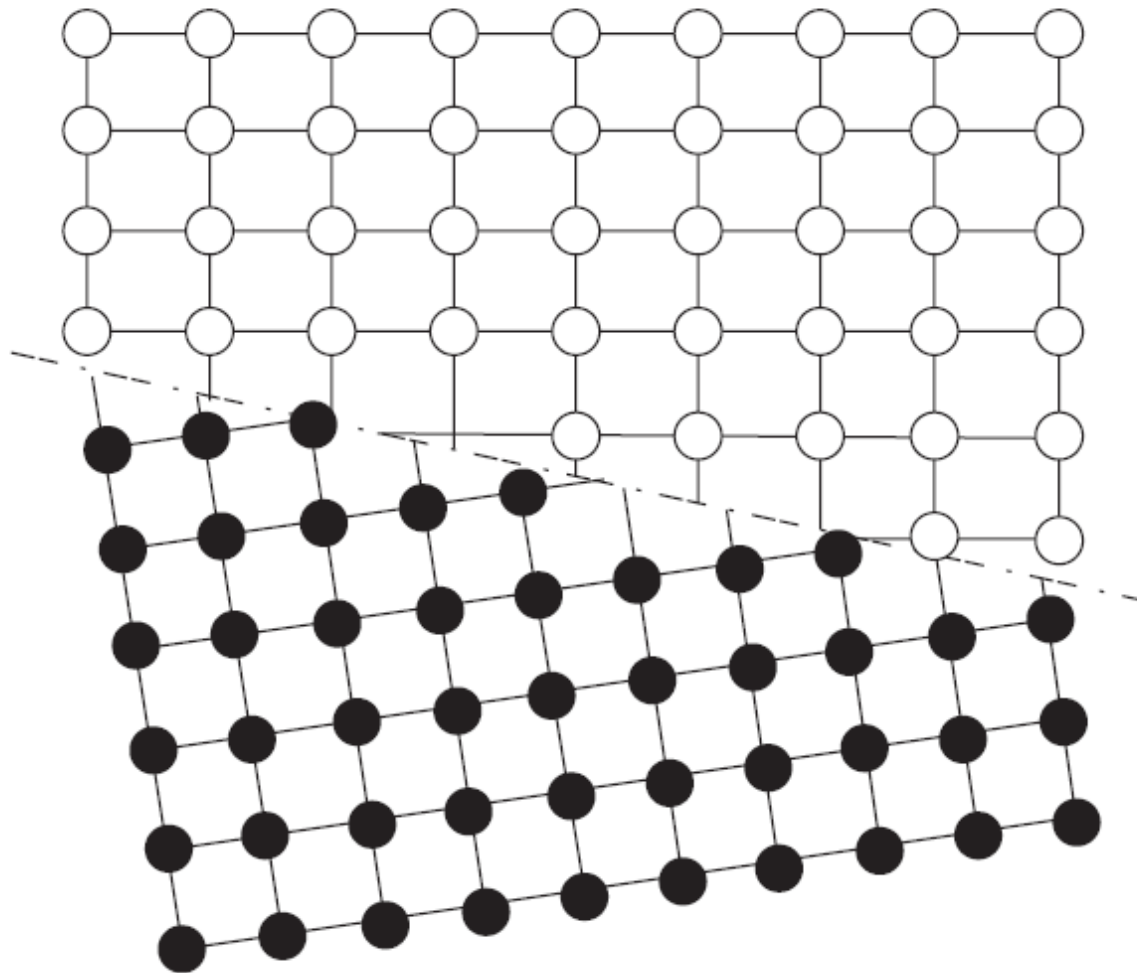
A-B bonds   misfit dislocation

A <u>semicoherent interface</u>. The misfit parallel to the interface is accommodated by a series of edge dislocations.

$$\delta = \frac{d_\beta - d_\alpha}{d_\alpha} \quad D = \frac{d_\beta}{\delta} \quad \begin{array}{l} \text{Interfacial energy} \\ \sim 200\text{-}500 \ \text{mJ m}^{-2} \end{array}$$
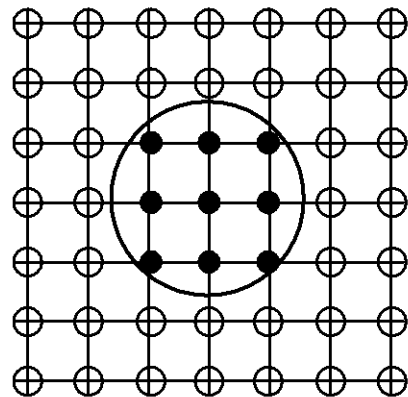
Interfacial energy: $\quad \gamma_{st} \propto 1/D \propto \delta$
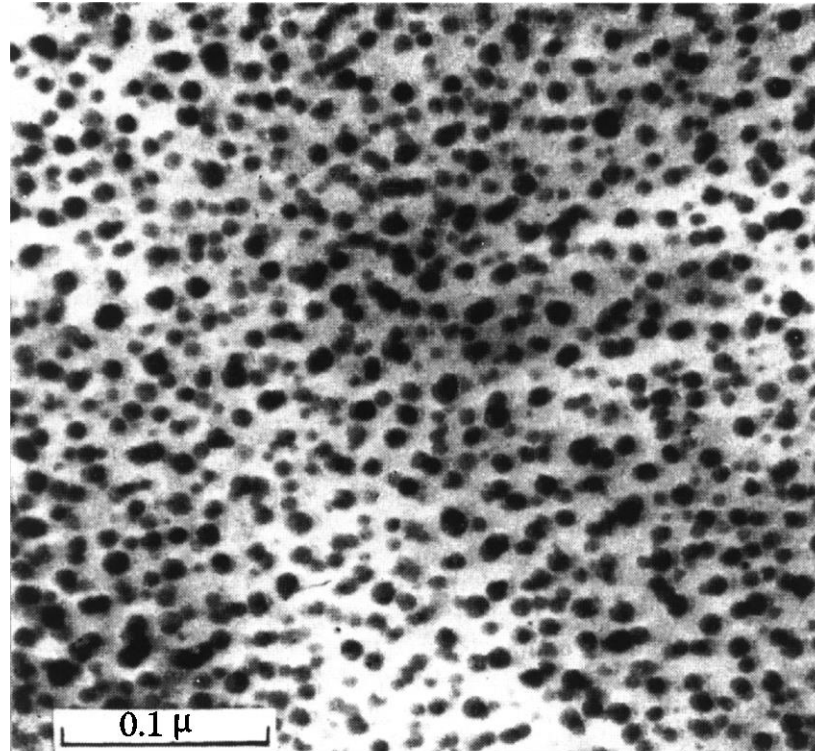
3.4 Interphase Interfaces in Solids

An <u>incoherent interface</u>. Interfacial plane has very different atomic configurations: Two randomly oriented crystals. High interfacial energy ~500-1000 mJ/m^2

3.4.2 Fully Coherent Precipitates

Ag rich ~10nm fcc regions

(a) A zone with no misfit ($\circ$ Al, $\bullet$ Ag, for example), (b) Electron micrograph of Ag-rich zones in an Al-4 atomic % Ag alloy ($\times$ 300 000), (After R.B. Nicholson, G. Thomas and J. Nutting, *Journal of the Institute of Metals,* **87** (1958-1959) 431.)
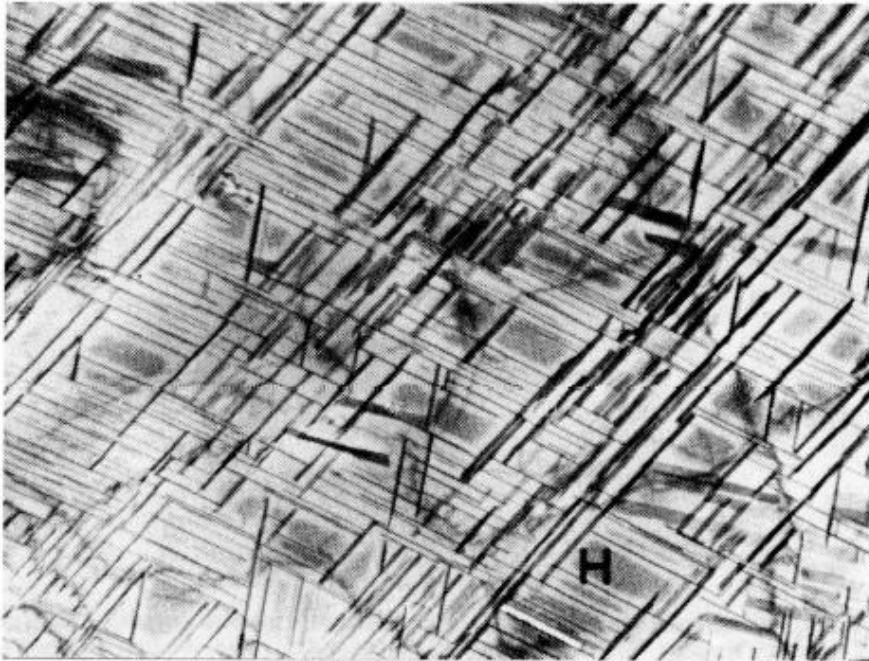
3.4.2 Interphase Interfaces

Fig. 3.42 Electron micrograph showing the Widmanstätten morphology of γ' precipitates in an Al-4 atomic % Ag alloy. GP zones can be seen between the γ', e.g. at H ($\times$ 7000). (R.B. Nicholson and J. Nutting, *Acta Metallurgica*, **9** (1961) 332.)

Partially coherent precipitates

Fig. 3.45 Possible morphologies for grain boundary precipitates. Incoherent interfaces smoothly curved. Coherent or semicoherent interfaces planar.

Grain-boundary precipitates

A **precipitate at a grain boundary triple point** in an $\alpha \rightleftharpoons \beta$ Cu-In alloy. Interfaces A and B are incoherent while C is semicoherent ($\times$ 310). (After G.A. Chadwick, *Metallography of Phase Transformations*, Butterworths, London, 1972.)
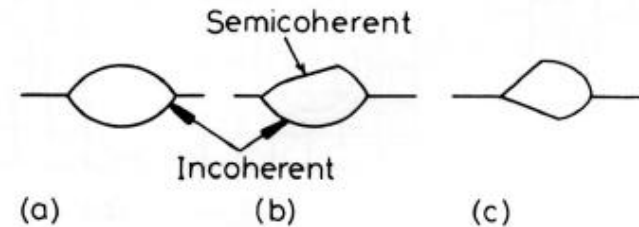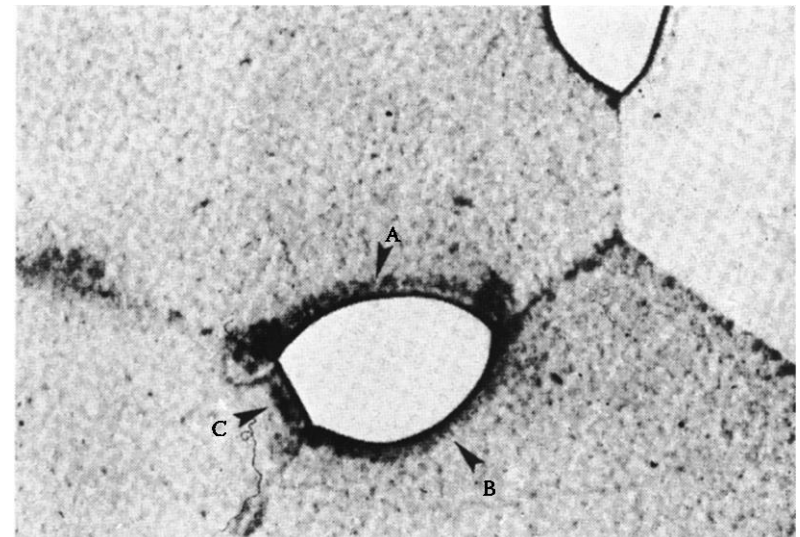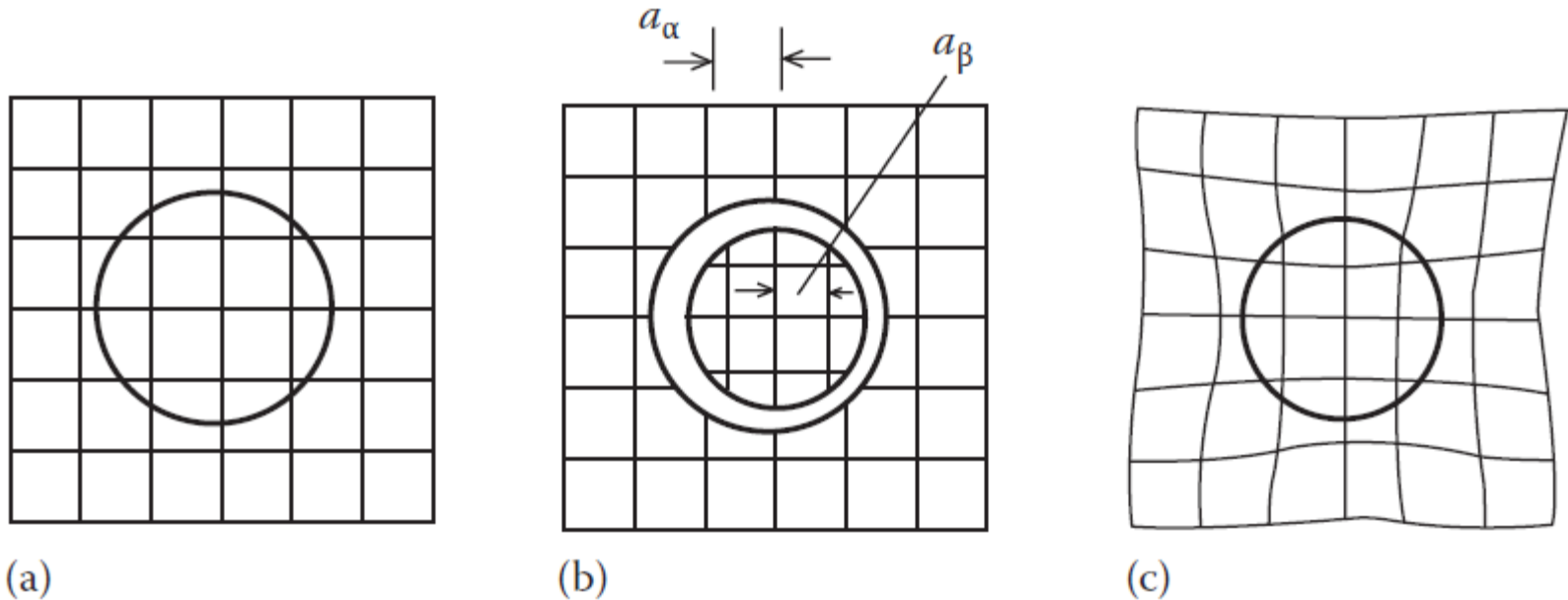
3.4.3 Second Phase Shape: Misfit Strain Effects

Fully coherent precipitates

The origin of coherency strains. The number of lattice points in the hole is conserved.

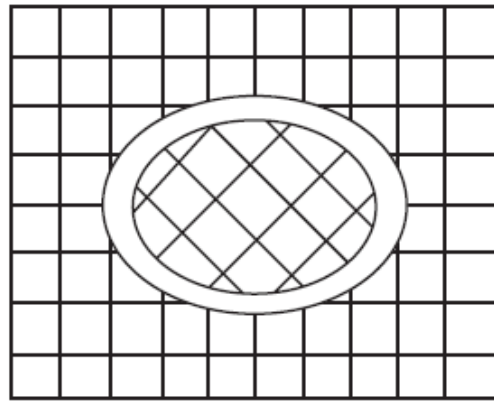$$\sum A_i \gamma_i + \Delta G_s = \text{minimum}$$

Interfacial energy   Elastic strain energy

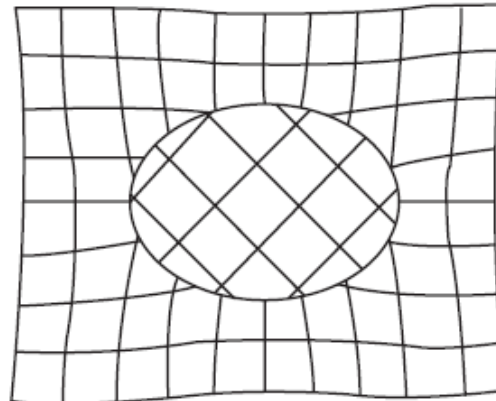Condition for mechanical equilibrium

$$\Delta G_s \approx 4\mu\, \delta^2 \cdot V$$

shear modulus of matrix   unconstrained misfit

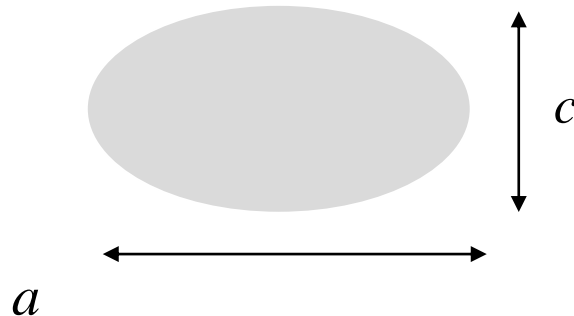# 3.4.3 Second Phase Shape: Misfit Strain Effects

(a)

(b)

The origin of misfit strain for an <u>incoherent inclusion</u> (no lattice matching).

incoherent precipitates = no coherency strains

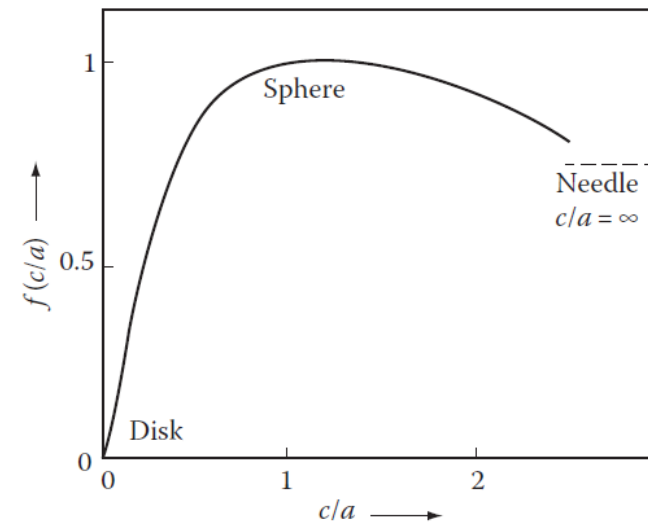Volume misfit: $\Delta = \dfrac{\Delta V}{V}$

$$\Delta G_s = \frac{2}{3}\mu\,\Delta^2 \cdot V \cdot f(c/a)$$

shear modulus of matrix

c

a

$$\sum A_i \gamma_i + \Delta G_s = \text{minimum}$$

No coherency strains

The variation of misfit strain energy with ellipsoid shape

3.4.3 Second Phase Shape: Coherency Loss

Coherent precipitates:

$$\Delta G_s \approx 4\mu\,\delta^2 \cdot \frac{4}{3}\pi r^3 + 4\pi r^2 \cdot \gamma_{ch}$$

coherency strains

Non-coherent precipitates:

$$\Delta G_s \approx 0 + 4\pi r^2(\gamma_{ch} + \gamma_{st})$$
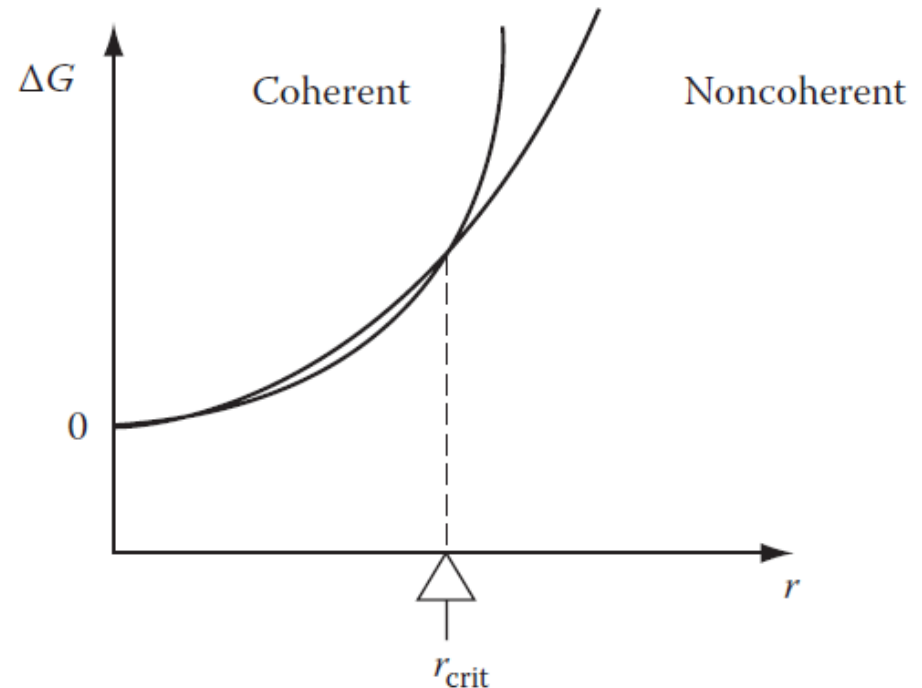
chemical interfacial energy

structural interfacial energy (due to misfit dislocations)
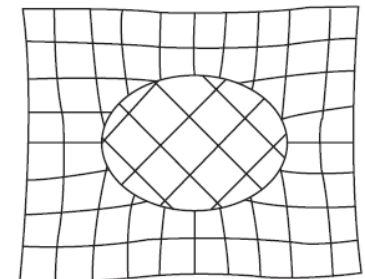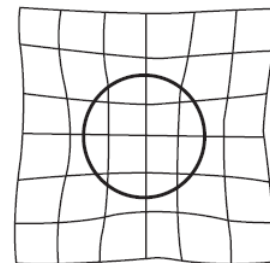
Critical radius:

$$r_{crit} = \frac{3\gamma_{st}}{4\mu\delta^2}$$

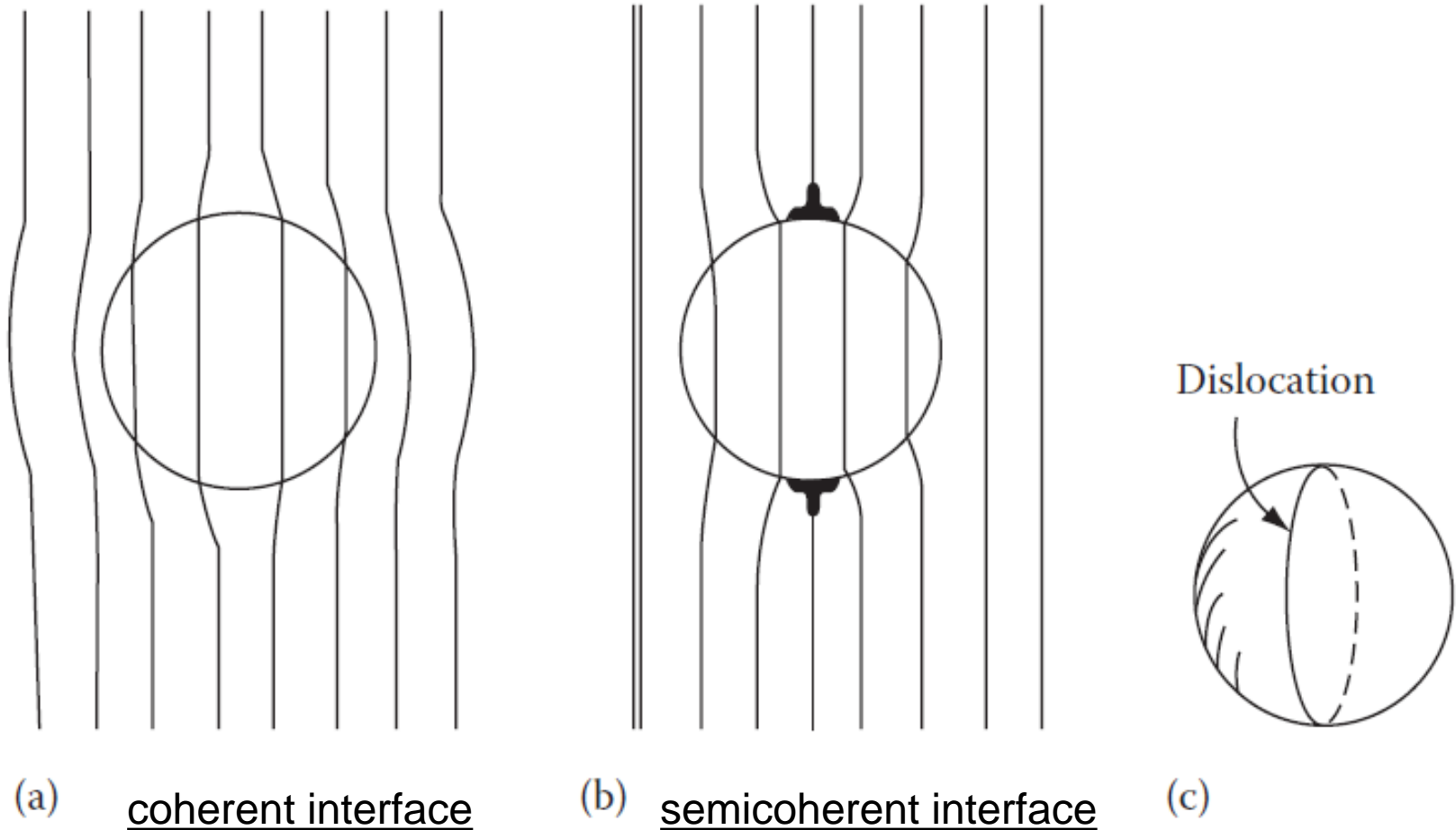Assuming: $\gamma_{st} \propto \delta$

$$r_{crit} \propto \frac{1}{\delta}$$

The total energy of matrix + precipitate versus precipitate radius for spherical coherent and non-coherent (semicoherent or incoherent) precipitates.

3.4.4 Coherency Loss: Dislocation loop

(a) coherent interface
(b) semicoherent interface
(c) Dislocation

Coherency loss for a spherical precipitate, (a) Coherent, (b) Coherency strains replaced by dislocation loop, (c) In perspective.

How does an amorphous solid fail?

- Flow of glassy materials is a paradigmatic topic in materials physics: polymers, amorphous metals, foams, emulsions, colloidal mixtures, yield stress fluids
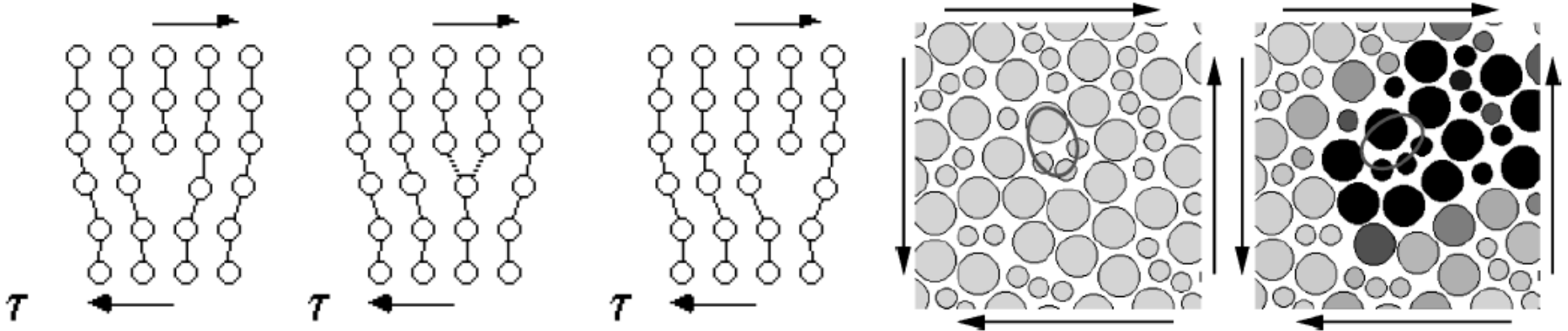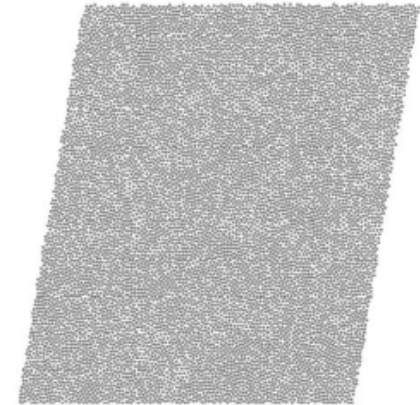
Falk and Langer, Phys Rev E (1998)

- In crystals, defects (dislocations) mediate plasticity

- In amorphous solids, there are local plastic events, but we cannot easily connect them to structural properties